TURKISH JOURNAL OF VETERINARY RESEARCH

Vol: 6 No:1
Year 2022
E-ISSN: 2602-3695

TJVR
http://dergipark.gov.tr/tjvr

TURKISH JOURNAL OF VETERINARY RESEARCH

E-ISSN:2602-3695

Year	Volume	Issue / Number
2022	6	1

All articles in this journal are available free of charge from
https://dergipark.org.tr/en/pub/tjvr

TJVR is published biannually

Indexing:

The Turkish Journal of Veterinary Research (TJVR) is indexed and abstracted by the following indexes and platforms (Alphabetical order); *Academic Keys, Asos Index, BASE, CABI Abstract, Crossref, EBSCO, Entire WEB, EuroPub, Genamics, Google Scholar, Ideal Online, Index Copernicus, IP Indexing, J-Gate, Journal TOCs, Open Access Library, Open AIRE, Pmi to Cite, Research BIB, Scholar Index, TRDizin, Turkiye Atıf Dizini, Udl Edge, Ulrichs Web, World Cat,.*

TURKISH JOURNAL OF VETERINARY RESEARCH
E-ISSN:2602-3695

Year	Volume	Issue / Number
2022	6	1

ORIGINAL ARTICLES

CASE REPORT

Original Article https://doi.org/10.47748/tjvr.993547

TJVR 2022; 6 (1): 1-8

Turkish Journal of Veterinary Research

https://dergipark.org.tr/tr/pub/tjvr

e-ISSN: 2602-3695

Investigation of 16S rRNA, *mecA* and *nuc* genes in coagulase-positive and negative Staphylococci by Real-Time PCR

Abdulbaki Aksakal[1] Şükrü Önalan[2] Şeyda Şilan Okalin[3]

[1] *Department of Pharmaceutical Microbiology, Faculty of Pharmacy, Adiyaman University, Adiyaman, Turkey*
[2] *Department of Fish Diseases, Faculty of Fisheries, Van Yuzuncu Yil University, Van, Turkey*
[3] *Department of Clinical Microbiology and Microbiology, Health Sciences Institute, Dokuz Eylul University, Izmir, Turkey*

Correspondence: *Şükrü Önalan (sukruonalan@yyu.edu.tr)*

Received: 10.09.2021 Accepted: 30.12.2021

ABSTRACT

Objective: *Staphylococcus aureus* is a Gram-positive and round-shaped bacterium. It is often positive for catalase and nitrate reduction. Pathogenic isolates support infections by producing protein toxins and the expression of a cell-surface protein virulence factors. Sepsis-related to methicillin-resistant *S. aureus* (MRSA) has significant morbidity and high mortality rates (15-30%). The methicillin resistance for *S. aureus* is coded with the *MecA* gene, while the methicillin sensitivity is coded with the *Nuc* gene, and they are chromosomal. Similarly, it is coded with the coagulase gene for *S. aureus* (*Coa*).

Materials and Methods: In this study, the 16S rRNA gene identification by Real-Time PCR was investigated in forty *S. aureus* isolates, which were cultured at different times in terms of MIC and SIR tests. The isolates used in the study were determined at the gene level in terms of their differences in methicillin resistance gene (*MecA*), methicillin susceptibility gene (*Nuc*), coagulase gene (*Coa*) and intra-species differences were examined.

Results: As a result of the study, *Staphylococcus* spp. yielded positive results with 16S rRNA gene-specific primers in all isolates. Real-Time PCR analysis of the isolates with SYBRGreen-based PCR analysis was performed with 16S rRNA gene-specific primers, and the samples were confirmed to be *Staphylococcus*. Analysis at the family level was followed by *Coa*, *Nuc*, and *MecA* gene Real-Time PCR results, and it was found that, in terms of *Coa* and *Nuc* genes, 19 isolates were positive and 21 isolates were negative. In terms of *MecA* gene, 16 isolates were positive according to the positive sigmoidal curves and to the single peak melting values, whereas 24 isolates were found to be negative.

Conclusion: It is thought that this study will benefit the community by contributing to the rapid and effective treatment and diagnosis of infections caused by coagulase-positive/negative *Staphylococci*.

Keywords: *Coagulase gene, MecA gene, Nuc gene, Staphylococcus aureus, 16S rRNA gene*

INTRODUCTION

S. aureus belongs to the family of *Micrococcaceae* and is grouped under the *Staphylococcus* genus. They are Gram-positive, oxidase-negative, catalase-positive, immobile, non-spore-producing, facultative anaerobe, round coce-shaped microorganisms. As cell division occurs at different planes, the cells are seen together in botryoid form in preparations. *S. aureus* can be produced in the usually used media, at a temperature of 37°C and pH 7.4. They form porcelain-shaped, convex, smooth-surfaced, often yellow-pigmented colonies in the blood gel

medium. Around the colonies, there are generally characteristic hemolysis zones (Levinson, 2002). Some studies carried out in recent years have aimed to increase the resistance of *S. aureus* antibiotics against Methicillin Resistant *Staphylococcus aureus* (MRSA). In studies carried out for this purpose, it has been reported that successful results have been achieved in molecular-based analyzes (Sharaf et al., 2021). In addition, it has been reported that *S. aureus*, the best-known food pathogen, was isolated from waste containers in food businesses and the presence of resistance genes was observed in molecular studies of isolated *S. aureus* isolates (Shahid et al., 2021).

The *Staphylococcus* family's pathogenicity is generally based on the ability to produce coagulase encoded by the *Coa* gene, and coagulase-negative staphylococci are considered secondary infectious pathogens. These bacteria have a huge variety of resistance genes and have more than 40 genes related to resistance in Staphylococci. Some resistance properties are provided by the *MecA* gene (Yadav et al., 2018). The *MecA* gene encodes methicillin resistance, and it is chromosomal. The *MecA* gene is found in all methicillin-resistant coagulase-negative Staphylococci (MRCNS) strains. Strains with this gene are resistant to all beta-lactams because they produce a new penicillin-binding protein (PBP). However, methicillin resistance is not always detectable in routine tests as it is affected by environmental conditions. Therefore, a methicillin-resistant *Staphylococci* can be identified as susceptible. Therefore, PCR is a useful and efficiently method with high sensitivity and specificity in determining methicillin resistance in Staphylococci (Willke et al., 2012). This study aimed at rapid and effective treatment and diagnosis of infections caused by coagulase positive/negative Staphylococci by molecular methods.

MATERIALS and METHODS

Bacterial strains. This study was carried out with the permission of the Local Ethics Committee of Faculty of Medicine, Non-Interventional Clinical Research Ethics Committee on 03.06.2016, and with decision number 09. *Staphylococcus* spp. isolates were isolated from culture samples taken at different times and in various regions in Turkey. Bacterial isolations were carried out on Blood (BA) Agar. Then, they are incubated at 37°C for 18-24 hours. Samples with colony growth were examined macroscopically and microscopically. Colonies suspected to be *Staphylococcus* spp. were identified using standard bacteriological methods (Gram staining, mobility, catalase, lamina, and tube coagulase test, DNase, mannitol fermentation). Accordingly, 20 coagulase-positive and 20 coagulase-negative *Staphylococci* spp. strains obtained as a result of lamina and tube coagulase tests were stored in 15% glycerol Trypticase Soy Broth (TSB) until the time of PCR procedure at -20°C (Bilgehan, 2002; Kaya et al., 2003; Tok and Coşkun, 2010; Nia et al., 2011). Biochemical identifications of the isolated strains, coagulase, and oxacillin MIC tests, and antibiotic susceptibilities were performed using the BD Phoenix™ Bacteria Identification and Antibiogram Device (Becton Dickinson, USA) by ID/AST Combo kit (Tok and Coşkun, 2010; Uçan, 2014). Total DNA isolation was performed using *Staphylococcus* spp. strains identified in routine procedures and extracts obtained in the culture medium. Molecular identification of bacteria was performed by Real-Time PCR for the 16S rRNA gene. For the molecular characterization of isolates, the *MecA* and *Nuc* genes were investigated. Coagulase results (*Coa*) were evaluated depending on *Mec* and *Nuc* gene results. Isolation of bacterial DNA from culture plates was performed with the QIAamp DNA mini kit (Qiagen). The DNA isolations were performed according to the manufacturer's instructions. Molecular steps were carried out with the support of Van Yuzuncu Yil University, Biotechnology Application and Research Center, and Van Yuzuncu Yil University Fisheries Faculty, Fish Disease Laboratories.

Bacterial identification and antibacterial activity. All isolates were individually adjusted to 0.5 optical density (OD). Bacterial suspensions were transferred in the BD Phoenix (Phoenix™ Automated Microbiology System-Becton Dickinson) identification kit. The kit was incubated for 18 hours at 37°C. The samples were evaluated for 26 antibiotics according to their Minimum Inhibition Concentration (MIC) and resistance (SIR) status (Önalan, 2019).

DNA Isolation. DNA isolations were performed using DNA Mini Kit (Qiagen) with QIAcube automatic isolation robot. The Real-Time PCR was carried out 25 µl total volume of specific forward and reverse primers (27F-1492R), SYBR Green-based qPCR Mastermix and water (Önalan and Yavuz, 2019).

Primers. For the identification of *Staphylococcus* spp. isolates, 16S rRNA gene region *Staphylococcus* spp. specific primers were used. The primer set was used as S16-F 5'-AGAGTTTGATCATGGCTCAG-3' and S16-R 5'-GGACTACCAGGGTATCTAAT-3', as reported by Özen et al., (2011). For the methicillin resistance of the isolates, the *MecA* gene, and for the coagulase positivity, the *MecA* gene results were evaluated together with the *Nuc* gene results. *MecA* and *Nuc* gene-specific primer sequences used in the study were used as *MecA*-F-5'-AAAATCGATGGTAAAGGTTGGC-3', *MecA*-R-5'-AGTTCTGCAGTACCGGATTTGC-3', *Nuc*-F-5'-GCGATTGATGGTGATACGGTT and *Nuc*-R 5'-AGCCAAGCCTTGACGAACTAAA-3' (Özen et al., 2011).

Real-Time PCR Analysis. In the Real-Time PCR, pre-denaturation was carried out at 95°C for 10 min. Then, 45 cycles were completed as denaturation at 94°C for 45 sec, annealing at 55°C for 30 sec, and extension at 72°C for 45 sec. Then as the last step, the last-extension process was carried out at 72°C for 7 minutes. Non-template control (NTC) tubes were used as a negative sample control. After analysis, sigmoidal curves have been evaluated as positive (Altinok et al., 2007).

RESULTS

In addition to 40 strains used in the study, *S. aureus* ATCC 25923, *S. aureus* ATCC 6538, and *S. aureus* ATCC 29213 strains were used as the controls for *MecA*, *Nuc*, and *Coa* genes. According to the lamina and tube coagulase test results, 20 samples that were coagulase-positive were identified as *S. aureus* while 20 samples that were coagulase-negative were identified as *Staphylococcus* spp. Ten of the coagulase-negative staphylococci were identified as *S. epidermidis*, 5 were identified as *S. haemolyticus*, 2 were identified as *S. auricularis* and, *S. hominis*, one was identified as *S. lugdunensis*, and one was identified as *S. warneri*. Coagulase results of coagulase-positive and negative *Staphylococci* spp. and oxacillin MIC values were determined in BD Phonenix™ 100 instrument. Accordingly, it was determined that one of the coagulase-positive *S. aureus* strains was Methicillin-Resistant *S. aureus* (MRSA). Methicillin-Resistant Coagulase Negative *Staphylococcus* (MRCNS) was detected in 15 coagulase-negative *Staphylococci* spp. (Table 1).

To determine *Staphylococcus* spp. isolates using molecular methods, PCR was performed with family-specific primers. For this purpose, forward (5'-AGAGTTTGATCATGGCTCAG-3') and reverse (5'-GGACTACCAGGGTATCTAAT-3') primers were used (Özen et al., 2011).

Table 1. Biochemical test results of isolates with methicillin, coagulase, cefoxitin and oxacillin.

No	Isolate name	Coagulase	Cefoxitin MIC	Oxacillin MIC	Methicillin
1	*S. aureus*	+	<=2	<=0.25	S
2	*S. aureus*	+	<=2	0.5	S
3	*S. aureus*	+	4	0.5	S
4	*S. aureus*	+	4	1	S
5	*S. aureus*	+	<=2	<=0.25	S
6	*S. aureus*	+	<=2	<=0.25	S
7	*S. aureus*	+	4	0.5	S
8	*S. aureus*	+	<=2	<=0.25	S
9	*S. aureus*	+	<=2	<=0.25	S
10	*S. aureus*	+	4	0.5	S
11	*S. aureus*	+	4	<=0.25	S
12	*S. aureus*	+	4	0.5	S
13	*S. aureus*	+	<=2	0.5	S
14	*S. aureus*	+	<=2	<=0.25	S
15	*S. aureus*	+	<=2	<=0.25	S
16	*S. aureus*	-	>8	>2	R
17	*S. aureus*	+	<=2	<=0.25	S
18	*S. aureus*	+	<=2	0.5	S
19	*S. aureus*	+	<=2	<=0.25	S
20	*S. aureus*	+	4	0.5	S
21	*S. epidermidis*	-	-	>2	R
22	*S. epidermidis*	-	-	>2	R
23	*S. epidermidis*	-	-	>2	R
24	*S. epidermidis*	-	-	>2	R
25	*S. epidermidis*	-	-	>2	R
26	*S. epidermidis*	-	-	>2	R
27	*S. epidermidis*	-	-	>2	R
28	*S. epidermidis*	-	-	1	R
29	*S. epidermidis*	-	-	<=0.25	S
30	*S. epidermidis*	-	-	<=0.25	S
31	*S. haemolyticus*	-	-	>2	R
32	*S. haemolyticus*	-	-	>2	R
33	*S. haemolyticus*	-	-	>2	R
34	*S. haemolyticus*	-	-	2	R
35	*S. haemolyticus*	-	-	<=0.25	S
36	*S. auricularis*	-	-	>2	R
37	*S. auricularis*	-	-	<=0.25	S
38	*S. hominis*	-	-	2	R
39	*S. lugdunensis*	-	-	>2	R
40	*S. warneri*	-	-	<=0.25	S

*S: Sensitive, R: Resistant, MIC: Minimal Inhibitory Concentration

S. aureus and *S. lugdunensis* with oxacillin MIC values<=2 mcg/mL and cefoxitin MIC values<=4 mcg/mL are mostly methicillin susceptible through

the absence of the *MecA* gene. Coagulase-negative staphylococci (except *S. lugdunensis*) with oxacillin MIC values of>0.25 mcg/mL are mostly methicillin resistant due to the presence of the *MecA* gene.

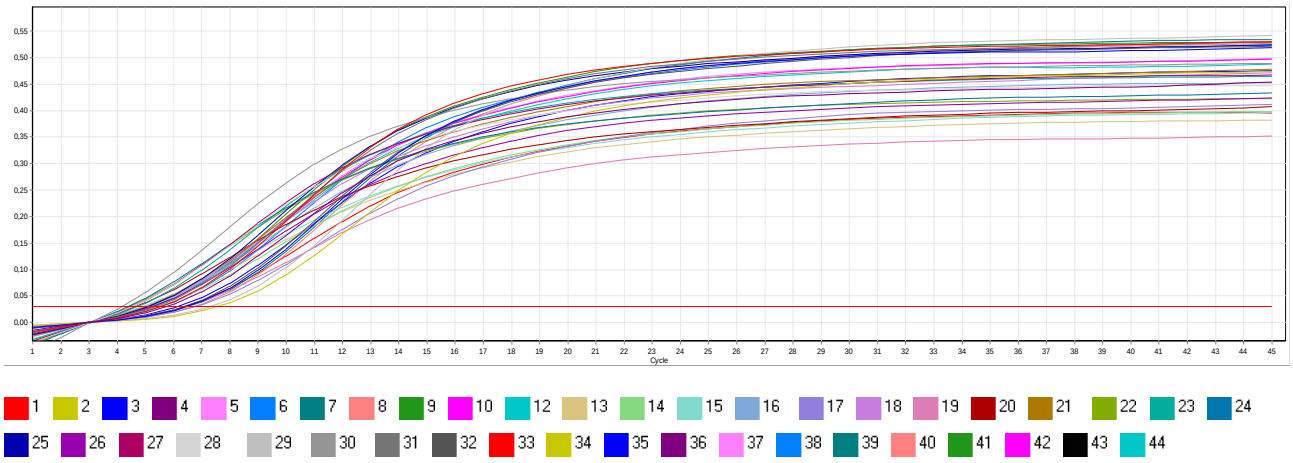

Figure 1. Real-Time PCR results with 16S rRNA gene-specific primers.

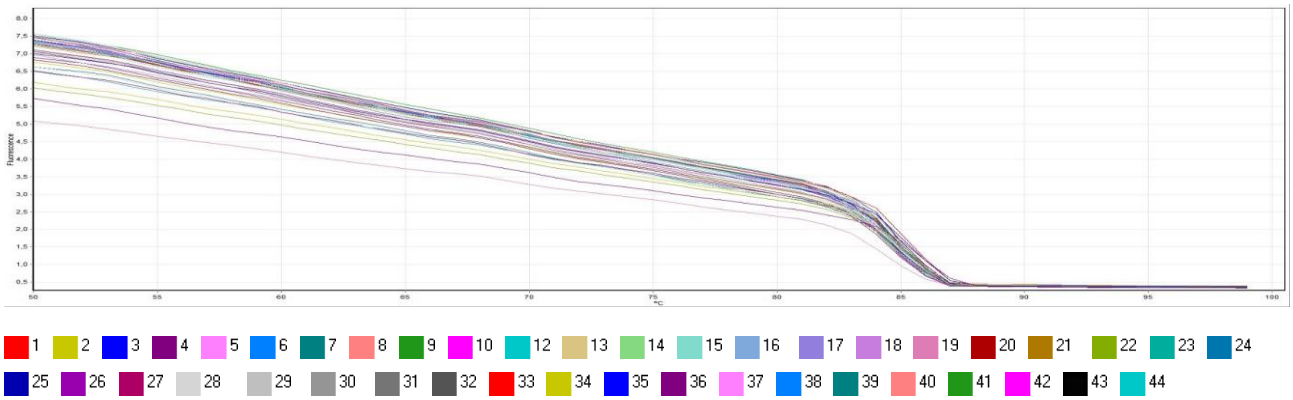

Figure 2. Real-Time PCR melting analysis result of 16S rRNA gene.

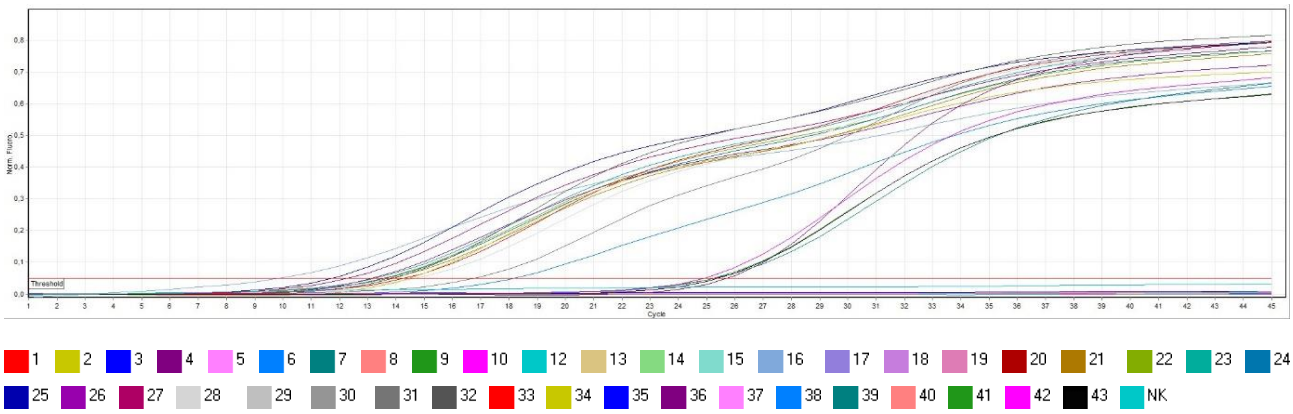

Figure 3. The results of Real-Time PCR with *MecA* gene-specific primers.

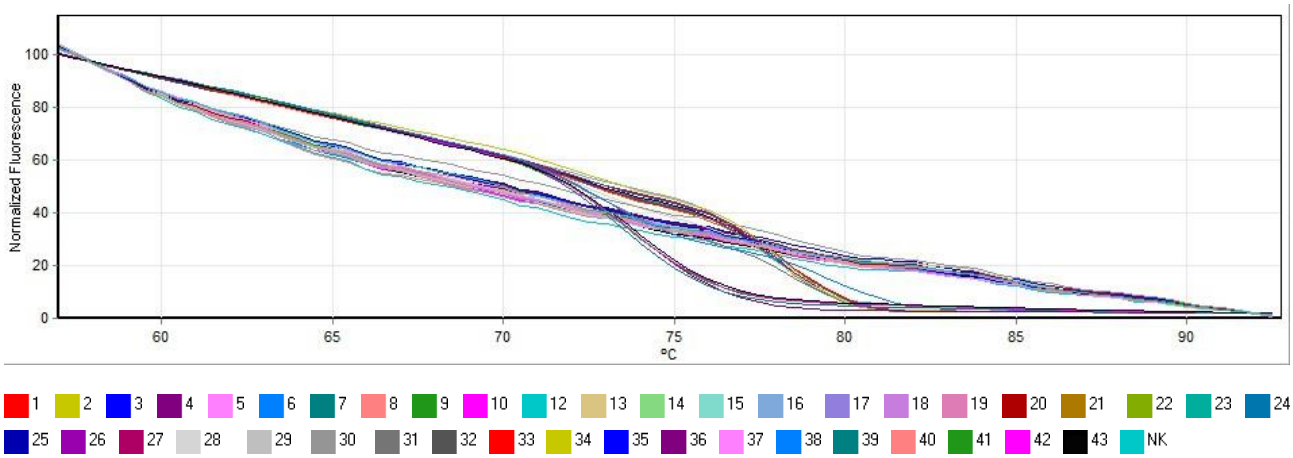

Figure 4. Real-Time PCR melting analysis result of *MecA* gene.

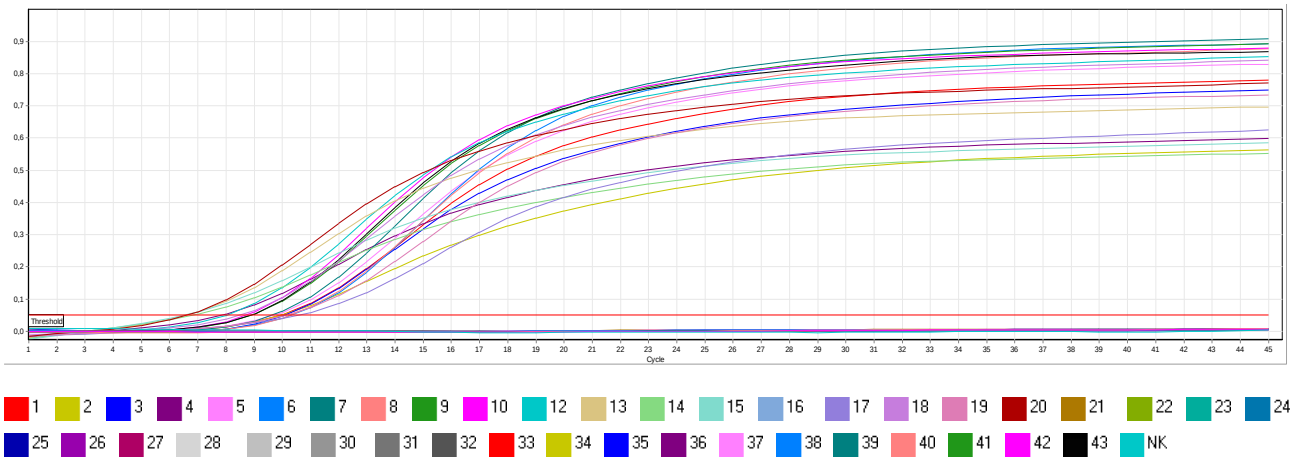

Figure 5. The results of the Real-Time PCR with *Nuc* gene-specific primers.

As a result of the Real-Time PCR procedure using SYBR Green qPCR mastermix (11.0 µl), forward (1.5 µl) and reverse (1.5 µl) primers, DNase, RNase, endotoxin-free water (9.0 µl) and template DNA (2.0 µl), the isolates were determined to be from the *Staphylococcus* family. In the optimized PCR protocol, following the pre-denaturation at 95°C, the 45 cycles performed at 94°C for 30 sec, 57°C for 20 seconds 72°C 30 sec. The final elongation was carried out at 72°C for 5 min to complete the PCR protocol. The results of Real-Time PCR with 16S rRNA gene-specific primers are given below (Figure 1).

After PCR, all strains used in the study showed positive results with 16S rRNA gene-specific primers, and they were identified as *Staphylococcus* spp. (Figure 1). After the Real-Time PCR processing, the accuracy of the study was confirmed by melting analysis. As a result of the melting analysis performed at 55-99°C, all samples started with 5-7.5 fluorescent irradiation and formed melting threshold peaks in the 83-87°C range. Based on these results, primers and PCR amplicon gave a standard melting curve, and all samples used in the study were verified (Figure 2).

Melting analysis showed that PCR amplicons melted in the same range, and similar PCR products were formed. Primers specific to the *MecA* gene (F-5'AAAATCGATGGTAAAGGTTGGC-3' and R-5'AGTTCTGCAGTACCGGATTTGC-3') were used to determine the methicillin resistance of the isolates. It was observed that 18 isolates that gave positive results from PCR were resistant to methicillin (Figure 3).

Accordingly, 18 (16, 21, 22, 23, 24, 25, 26, 27, 28, 31, 32, 33, 34, 36, 38, 39, 41, 42) isolates showed positive results on Real-Time PCR and the gene was evaluated to be positive. After the PCR procedure specific to the *MecA* gene, High-Resolution Melting (HRM) analysis was

performed, and the accuracy of the chemical and the method used in the study was confirmed. High resolution melting graph is given below (Figure 4).

Table 2. 16S rRNA, *Mec A*, *Nuc* and Coagulase gene characteristics of isolates used in this study.

No	Isolate Name	16S rRNA	Coagulase	Nuc gene	MecA gene
1	*S. aureus*	+	+	+	-
2	*S. aureus*	+	+	+	-
3	*S. aureus*	+	+	+	-
4	*S. aureus*	+	+	+	-
5	*S. aureus*	+	+	+	-
6	*S. aureus*	+	+	+	-
7	*S. aureus*	+	+	+	-
8	*S. aureus*	+	+	+	-
9	*S. aureus*	+	+	+	-
10	*S. aureus*	+	+	+	-
11	*S. aureus*	+	+	+	-
12	*S. aureus*	+	+	+	-
13	*S. aureus*	+	+	+	-
14	*S. aureus*	+	+	+	-
15	*S. aureus*	+	+	+	-
16	*S. aureus*	+	+	-	+
17	*S. aureus*	+	+	+	-
18	*S. aureus*	+	+	+	-
19	*S. aureus*	+	+	+	-
20	*S. aureus*	+	+	+	-
21	*S. epidermidis*	+	-	-	+
22	*S. epidermidis*	+	-	-	+
23	*S. epidermidis*	+	-	-	+
24	*S. epidermidis*	+	-	-	+
25	*S. epidermidis*	+	-	-	+
26	*S. epidermidis*	+	-	-	+
27	*S. epidermidis*	+	-	-	+
28	*S. epidermidis*	+	-	-	+
29	*S. epidermidis*	+	-	-	-
30	*S. epidermidis*	+	-	-	-
31	*S. haemolyticus*	+	-	-	+
32	*S. haemolyticus*	+	-	-	+
33	*S. haemolyticus*	+	-	-	+
34	*S. haemolyticus*	+	-	-	+
35	*S. haemolyticus*	+	-	-	-
36	*S. auricularis*	+	-	-	+
37	*S. auricularis*	+	-	-	-
38	*S. hominis*	+	-	-	+
39	*S. lugdunensis*	+	-	-	+
40	*S. warneri*	+	-	-	-
41	*S. aureus* ATCC-25923	+	+	+	+
42	*S. aureus* ATCC-6538	+	+	-	+
43	*S. aureus* ATCC-29213	+	-	+	-

The *Nuc* and *MecA* genes were evaluated together in the method used to determine the coagulase-positive or negative isolates used in the study. Positive and negative results obtained at the end of the PCR analyses using the *Nuc* gene-specific primer sets (F-5'GCGATTGATGGTGATACGGTT and R-5'AGCCAAGCCTTGACGAACTAAA-3') were evaluated together with the *Mec* gene results. The results of the isolates used the *Nuc* gene are given below (Figure 5).

Accordingly, 21 Nuc genes that yielded positive results in Real-Time PCR graph were evaluated as positive. The Real-Time PCR results of 16S rRNA, *Mec A*, *Nuc* and Coagulase results are as follows (Table 2).

According to the SYBR Green-based gene-level Real-Time PCR study results, all isolates were found to be positive for the 16S rRNA gene region-specific primers and were confirmed to be *Staphylococcus*. After the 16S rRNA PCR analysis performed at the family level, the coagulase results were determined together with the Real-Time PCR results for *Nuc* and *MecA* genes. Accordingly, 19 isolates were found to be positive, and 21 isolates were negative in terms of *Coa* and *Nuc* genes. In terms of the *MecA* gene, 16 isolates were positive according to the positive sigmoidal curves and to the single peak melting values, whereas 24 isolates were found to be negative. These results were observed to be in line with the biochemical results.

DISCUSSION

Staphylococcus species are characterized by their biochemical profiles, colony appearance, and hemolytic patterns. These Gram-positive bacteria are biochemically catalase-positive and oxidase-negative, and they use maltose. *S. aureus* produces virulent factors in various types including capsules, enzymes including adhesins, coagulase, catalase, hyaluronidase, staphylokinase, toxins including a toxin, β toxin, δ toxin, leukocidin, enterotoxin, exophilic toxins and toxic shock syndrome toxins causing various diseases in humans and animals (Javid et al., 2018). In a study on methicillin resistance, Seidel et al. (2017) aimed to carry out a rapid and accurate identification of *MecA* and *MecC* genes using nucleic acid lateral flow immunoassay (NALFIA) technology. Examination of 60 identified strains (MRS and non-target bacteria) and 28 methicillin-resistant *S. aureus* (MRSA) isolates from clinical samples was performed by NALFIA, classical PCR-gel electrophoresis and Real-Time PCR and the results were compared. It has been reported that NALFIA was superior to the other methods according to

detection limits, and differentiation between *MecA* and *MecC* can be made by displaying two different alleles on NALFIA test strips.

In this study, biochemical and antimicrobial properties of strains were identified by the BD Phonex ID. Similarly, Nasution et al. (2018) aimed to determine the *MecA* gene and antibiotic resistance pathway in 40 *S. aureus* isolates classified Methicillin-Resistant *S. aureus* (MRSA) by Vitek 2 Compact. The amplification of the *MecA* gene was performed by PCR and showed that all MRSA isolates had a 533 bp *MecA* gene. The antibiotic test of the Vitek 2 Compact showed that, although all isolates were resistant to beta-lactam group antibiotics, they had multiple drug resistance to other common antibiotics such as aminoglycosides, macrolides, and fluoroquinolones. However, the isolates were still susceptible to vancomycin (82.5% isolate), linezolid (97.5% isolate), and tigecycline (100% isolate).

In this study, Real-Time PCR was performed using gene-specific primers. As a result of this process, the isolates used in the study were identified to be from the same family by the 16S rRNA gene. Following this process, Real-Time PCR analyses were performed with *MecA* and *Nuc* genes. As a result, the coagulase properties of isolates were determined according to positive and negative results of *MecA* and *Nuc* genes. The analyses were carried out with *S. aureus, S. epidermidis, S. haemolyticus, S. auricularis, S. hominis, S. lugdunensis,* and *S. warneri* isolates and the reference bacteria (ATCC 25923, ATCC-6538, ATCC-29213). HRM test was used to determine the correct positivity and avoid false-positive results in Real-Time PCR analysis. As a result of this test, the accuracy of the procedures was determined by similar peaks given at ordinary temperatures. Similarly, many studies were conducted adopting identification by PCR. Elhassan et al. (2015) aimed to determine the prevalence of the *MecA* gene using the polymerase chain reaction in methicillin-resistant *S. aureus* (MRSA) isolates and to compare the results with those obtained by the conventional method. In this context, 200 *S. aureus* isolates were taken from patients with different diseases. The phenotypic Kirby-Bauer method, by adopting the E-test, confirmed that methicillin resistance was present in 61.5% of isolates with MICs ranging from 4 μg/mL to 256 μg/mL. Ashraf et al. (2014) aimed to determine *S. aureus*-specific thermonuclease gene (*Nuc*) in chickens by the Real-Time PCR test. The isolated *S. aureus* was susceptible to vancomycin, amoxicillin+clavulanic acid, and cephalothin, respectively, up to 84.5%, 83.8%, and 78.4%, and resistant to ampicillin, oxacillin, and penicillin up to 75%, 73%, and 70.2%, respectively. Hoegh et al. (2014) showed that variations in the *S. aureus*-specific *Nuc* gene could lead to misidentification of methicillin-sensitive and resistant *S. aureus*. Accordingly, in 10 *S. aureus* isolates, Real-Time PCR was performed with primers and probes that were designed explicitly for *Nuc* and *MecA* genes, and a DNA sequence analysis was performed. Hamidi et al. (2015) aimed to determine the prevalence of the production of coagulase (*Coa*) and thermonuclease (*Nuc*) genes and Staphylococcal enterotoxin A (*Sea*) among *S. aureus* samples isolated from various sources. In total, 100 *S. aureus* were isolated from 40 humans, 30 animals, and 30 food samples, and *Coa*, *Nuc*, and *Sea* genes were evaluated by the PCR. According to the culture results, Willke et al. (2012) have reported that of the 48 staphylococci strains, 15 were methicillin-resistant coagulase-negative Staphylococci (MRCNS), 4 were methicillin-resistant *S. aureus* (MRSA), and 14 were methicillin-sensitive coagulase-negative Staphylococci (MSCNS) and 15 were methicillin-sensitive *S. aureus* (MSSA). According to the PCR results, 17 of the strains were found to be MRCNS, 8 were found to be MRSA, 10 were found to be MSCNS and 13 were found to be MSSA. Levi and Towner (2003) have reported that 17 of the 200 blood cultures suspected of containing *Staphylococcus* were found to be positive by PCR, and 16 were found to be positive by culture method.

CONCLUSION

As a result of this study, the results of Real-Time PCR and BD Phoenix ID automatic devices were compared, and were found to be in agreement. It was thought that this study would benefit the community by contributing to the rapid and effective diagnosis and treatment of infections caused by coagulase-positive and negative Staphylococci.

ACKNOWLEDGMENTS

Compliance with Ethical Standards: The article does not contain any studies involving animals or humans performed by any of the authors.

Conflict of Interests: The authors declared that there is no conflict of interests.

Financial Disclosure: The authors declared that this study has received no financial support.

Author's Contributions: AA and ŞŞO designed the study. AA and ŞŞO performed surgeries. ŞÖ performed molecular analysis from bacteria. AA and ŞÖ performed statistical analysis. AA and ŞÖ participated in drafting and revising the manuscript. AA: Abdulbaki Aksakal, ŞÖ: Şükrü Önalan, ŞŞO: Şeyda Şilan Okalin

REFERENCES

Altinok I, Balta F, Capkin E, Kayis S. Disease of rainbow trout caused by *Pseudomonas luteola*. Aquaculture. 2007; 273(4):393-397.

Ashraf A, Hanan AF, Fatma I, Abdelhalim A. Detection of species-specific gene thermo nuclease (*Nuc*) in *Staphylococcus aureus* from chickens by Real-Time PCR assay. BVMJ. 2014; 27(2):415-422.

Bilgehan H. Clinical microbiological diagnosis, methods of examining microbiological morphology. İstanbul: Barış Publications; 2002.

Elhassan MM, Ozbak HA, Hemeg HA, Elmekki MA, Ahmed LM. Absence of the *MecA* gene in methicillin resistant *Staphylococcus aureus* isolated from different clinical specimens in shendi city, Sudan. Biomed Res Int. 2015; 1(1):1-5.

Hamidi RM, Hosseinzadeh S, Shekarforoush SS, Poormontaseri M, Derakhshandeh A. Association between the enterotoxin production and presence of *Coa, Nuc* genes among *Staphylococcus aureus* isolated from various sources, in Shiraz. Iran J Vet Res. 2015; 16(4):381-384.

Hoegh SV, Skov MN, Boye K, Worning P, Jensen TG, Kemp M. Variations in the *Staphylococcus aureus*-specific *Nuc* gene can potentially lead to misidentification of meticillin-susceptible and-resistant *S. aureus*. J Med Microbiol. 2014; 63(7):1020-1022.

Javid F, Taku A, Bhat MA, Badroo GA, Mudasir M, Sofi TA. Molecular typing of *Staphylococcus aureus* based on coagulase gene. Vet World. 2018;11(4):423-430.

Kaya E, Kırmalı O, Doğan Ö, Berk D, Kaya D. The susceptibility of ampicillin and ampicillin-sulbactam to bacteria with chronicotitis media. Türk Mikrobiyol Cem Derg. 2003; 33(1):115-117.

Levi K, Towner K. Detection of Methicillin-Resistant *Staphylococcus aureus* (MRSA) in blood with the EVIGENE MRSA Detection Kit. J Clin Microbiol. 2003; 41(8):3890-3892.

Levinson W. Medical microbiology & immunology. Ankara: Güneş Bookstore; 2002.

Nasution GS, Suryanto D, Kusumawati RL. Detection of *MecA* gene from methicillin resistant *Staphylococcus aureus* isolates of North sumatera. *InIOP Conference Series:* Environ Earth Sci. 2018; 130(1):1-7.

Nia KM, Sepehri G, Khatmi H, Shakibaie MR. Isolation and antimicrobial susceptibility of bacteria from chronic suppurative otitis media patients in Kerman, Iran. Iran Red Crescent Med J. 2011; 13(12):891-894.

Önalan Ş. Expression differences of stress and immunity genes in rainbow trout (*Oncorhynchus mykiss*, Walbaum 1792) with different bacterial fish diseases. Sr J Aquacult-Bamidgeh. 2019; 1537(1):1-10.

Önalan Ş, Yavuz Hİ. Spectrophotometric determination of development differences of *Lactococcus garvieae* isolates in liquid media containing nanoparticles. Menba Journal of Fisheries Faculty. 2019; 1(1):6-15.

Özen NS, Dağlar D, Baysan BÖ, *et al.* Evaluation of MRSA id chromogenic media in detecting methicillin resistant *Staphylococcus aureus* strains. Ankem Derg. 2011; 25(1):31-34.

Seidel C, Peters S, Eschbach E, Feßler AT, Oberheitmann B, Schwarz S. Development of a nucleic acid lateral flow immunoassay (NALFIA) for reliable, simple and rapid detection of the methicillin resistance genes *MecA* and *MecC*. Vet Microbiol. 2017; 200(1):101-106.

Shahid AH, Nazir KNH, El Zowalaty ME, *et al.* Molecular detection of vancomycin and methicillin resistance in *Staphylococcus aureus* isolated from food processing environments. One Health. 2021; 13(1):1-5.

Sharaf MH, El-Sherbiny GM, Moghannem SA, *et al.* New combination approaches to combat methicillin-resistant *Staphylococcus aureus* (MRSA). Scientific Reports. 2021; 11(1):1-16.

Tok D, Coşkun Ö. Antibiotic susceptibilities of microorganisms growing in the cultures of patients with chronicotitis media. TAF Prev Med Bull. 2010; 9(1):51-54.

Uçan N. Determination of coagulase negative staphylococci and goat antibiotic resistance in goats with subclinical mastitis (Master Thesis). Aydın: Adnan Menderes University, Institute of Health Sciences, 2014.

Willke A, Sayan M, Meriç M, Mutlu M. Early diagnosis of methicillin resistance in Real-Time PCR in *Staphylococci* growing in blood cultures. Microbiyol Bul. 2012; 46(4):671-675.

Yadav R, Kumar A, Singh V, Singh J, Yadav SK. Molecular determination of methicillin resistance *MecA* and virulence *Coa* genes in *Staphylococcus aureus* from pyogenic clinical cases of companion animals in India. Turk J Vet Anim Sci. 2018; 42(5):371-375.

Original Article https://doi.org/10.47748/tjvr.1037041

TJVR 2022; 6 (1): 9-14

Turkish Journal of Veterinary Research

https://dergipark.org.tr/tr/pub/tjvr

e-ISSN: 2602-3695

Immunohistochemical detection of pro-inflammatory and anti-inflammatory interleukins in the lungs of sheep with jaagsiekte

Emin Karakurt[1] Enver Beytut[1] Serpil Dağ[1] Hilmi Nuhoğlu[1] Ayfer Yıldız[1] Emre Kurtbaş[2]

[1] *Department of Pathology, Faculty of Veterinary Medicine, Kafkas University, Kars, Turkey*
[2] *Institute Health Sciences, Kafkas University, Kars, Turkey*

Correspondence: *Emin Karakurt (mehmeteminkarakurt@hotmail.com)*

Received: 15.12.2021 Accepted: 25.01.2022

ABSTRACT

Objective: In this study, it was aimed to evaluate the levels of interleukins such as IL-1β, IL-6, IL-10 and IL-12β in sheep with Jaagsiekte by immunohistochemical methods. In this way, it will be revealed whether interleukins are effective in the progression of Jaagsiekte and how useful they are in the diagnosis of the disease.

Material-Method: The material of the current study consisted of lung tissues of 26 sheep (Control, n=6 and Jaagsiekte, n=20) brought to the Department of Pathology for routine histopathological diagnosis. Tissue samples taken were fixed in 10% buffered formaldehyde solution. 5 µm-thick sections were taken from the paraffin blocks prepared after routine tissue follow-up procedures. Hematoxylin & Eosin staining was applied to the sections in order to detect histopathological changes. Sections were examined and photographed under a light microscope. The routine streptavidin–biotin peroxidase complex method was used.

Results: In sheep with Jaagsiekte, tumoral foci with large and small acinar or papillary growths were observed in the alveolar and bronchiole lumens. The control group was negative for IL-1β, IL-6, IL-10 and IL-12β immunoreactivity. IL 1β-6-10 and 12β levels were dramatically increased in the Jaagsiekte group compared to the control group.

Conclusion: It was determined that interleukins were produced from tumoral cells and tumor microenvironment elements, and these interleukins showed pro-inflammatory effects, except for IL-10.

Keywords: *Jaagsiekte, Interleukins, Sheep*

INTRODUCTION

Jaagsiekte, also known as ovine pulmonary adenocarcinoma (OPA), is a contagious lung cancer of sheep and goats, caused by Jaagsiekte Sheep Retrovirus (JSRV) (Gomes et al., 2017; Lee et al., 2017). Jaagsiekte occurs worldwide in almost all countries except in New Zealand and Australia (Belalmi et al., 2020). The tumor originates from type 2 pneumocytes and Clara cells and shows many similarities in histological features to human pulmonary adenocarcinomas (Scott et al., 2018; Toma et al., 2020).

Cytokines, such as interleukin (IL), interferon (IFN) and tumor necrosis factor (TNF), which are important signaling proteins act as important mediators of the immune system. Expression levels, polymorphisms or profiles of cytokines and cytokine receptors can affect the pathogenesis of

virus-related diseases (Larruskain and Jugo 2013; Ding et al., 2021).

Interleukin 1 beta (IL-1β), a proinflammatory cytokine, regulates the expression of genes involved in various inflammatory processes and plays a central role in many chronic inflammatory diseases, including lung cancer such as non-small cell lung cancer (NSCLC) (Kim et al., 2013; Bhat et al., 2014). Increased expression of IL-1β in the tumor microenvironment correlates with poor prognosis in human lung adenocarcinomas (Tekpli et al., 2013; Ding et al., 2021).

Interleukin 6 (IL-6), a multifunctional proinflammatory cytokine, is produced by different cells, including immune cells, endothelial cells, cancer-associated fibroblasts, and tumor cells (Islas-Vazquez et al., 2020; Dutkowska et al., 2021). IL-6 is involved in the regulation of tumorigenesis, progression, and metastasis and its overexpression is particularly strongly associated with a poor prognosis for NSCLC (Kiss et al., 2020; Pan et al., 2020; Su et al., 2020).

Interleukin 10 (IL-10), an anti-inflammatory and protumoral effective cytokine, is mostly produced by M2-macrophages, T regulator cells (Tregs), Th2-cells, CD8+ T cells (Vahl et al., 2017; Gao et al., 2020). Il-10 can promote cancer development by suppressing macrophage function and allowing tumors to evade immune surveillance. Also the expression of IL-10 by tumor-associated macrophages (TAMs) correlates with unfavorable prognosis in NSCLC (Hsu et al., 2016; Pang et al., 2017; Hu et al., 2020).

Interleukin 12 (IL-12), an important immune regulatory cytokine, plays a role in stimulating Natural killer (NK) and T cell proliferation, increasing NK and CD8+ T cell cytolytic activity, and inducing various cytokines such as IFN-gamma (Yue et al., 2016). IL-12 exhibits immunostimulating and anti-angiogenic effects in promoting antitumoral immunity (Airoldi et al., 2009; D'Amico et al., 2012).

In this study, it was aimed to evaluate the levels of interleukins such as IL-1β, IL-6, IL-10 and IL-12β in sheep with Jaagsiekte by immunohistochemical methods. In this way, it will be revealed whether interleukins are effective in the progression of Jaagsiekte and how useful they are in the diagnosis of the disease.

MATERIALS and METHODS

Ethical Approval

This study was approved by the Kafkas University Animal Experiments Local Ethics Committee (KAU-HADYEK-2021/109).

Animals

The material of the current study consisted of lung tissue samples of 26 sheep (Control, n=6 and Jaagsiekte, n=20) brought to Veterinary Faculty, Department of Pathology for routine histopathological diagnosis.

Histopathological Examinations

Lung tissues were fixed in 10% neutral buffered formalin and routinely processed. Following routine procedures, tissues were embedded in paraffin wax. Paraffin sections of 5 μm thickness were stained with Hematoxylin & Eosin (H&E) to detect histopathological changes. Sections were examined under a light microscope and photographed.

Immunohistochemical Examinations

The routine streptavidin–biotin peroxidase complex method was used according to the manual instructions of the kit (Thermo Scientific Histostain-Plus IHC Kit, HRP, broad spectrum, REF: TP-125-HL). Anti-IL1β antibody (MyBioSource, MBS2026862, Polyclonal, Dilution Ratio: 1/50), anti-IL6 antibody (MyBioSource, MBS2012740, Monoclonal, Dilution Ratio: 1/100), anti-IL10 antibody (MyBioSource, MBS2026258, Polyclonal, Dilution Ratio: 1/200) and anti-12β (MyBioSource, MBS1490500, Polyclonal, Dilution Ratio: 1/50) were used after antigen retrieval and nonspecific protein blocking. The reactions were detected with aminoethyl carbazole (AEC) chromogen (Thermo Scientific, TA-125-HA). Counterstainings were conducted using hematoxylin. After this procedure, glass slides were mounted with Entellan and a coverslip. For control sections, PBS was applied in drops on the sections instead of the primary antibodies.

Prepared slides were examined under a light microscope (Olympus Bx53) and photographed via the Cell^P program (Olympus Soft Imaging Solutions GmbH, 3,4). Analyzes of the images were done with Image J Program (1.51j8). IL-1β, 6, 10 and 12β expressions were analysed by examining ten representative fields of labeled immune positive cells with the 40X magnification. Rating system were designated as negative (-) 0%,

weak (+) 1-10%, mild (++) 11-59% or severe (+++)>60%.

Statistical Analysis

Statistical analysis of the results was performed using the SPSS® (SPSS 26.0, Chicago, IL, USA) program. According to cell infiltration scoring, Kruskal-Wallis H test was used for multiple comparisons of IL-1β, IL-6, IL-10 and IL-12β, and Mann-Whitney U test was used for pairwise comparisons. Obtained results were given as mean ± standard error (SE). $P<0.05$ expression was considered statistically significant in the evaluation of the results.

RESULTS

Histopathological Findings

No pathological lesions were detected in the lung tissue of the healthy control group. In Jaagsiekte cases, tumoral foci with large and small acinar or papillary growths were observed in the alveolar and bronchiole lumens. A large number of alveolar macrophages were detected around these tumoral foci (Figure 1).

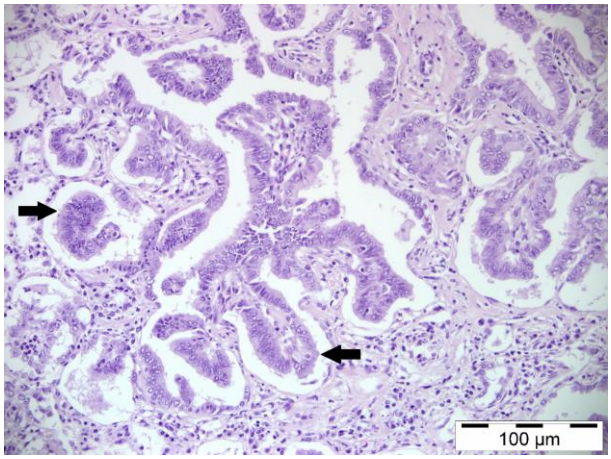

Figure 1. Lung, Neoplastic proliferations (arrows) within the alveolar lumen, H&E, Bar= 100 µm

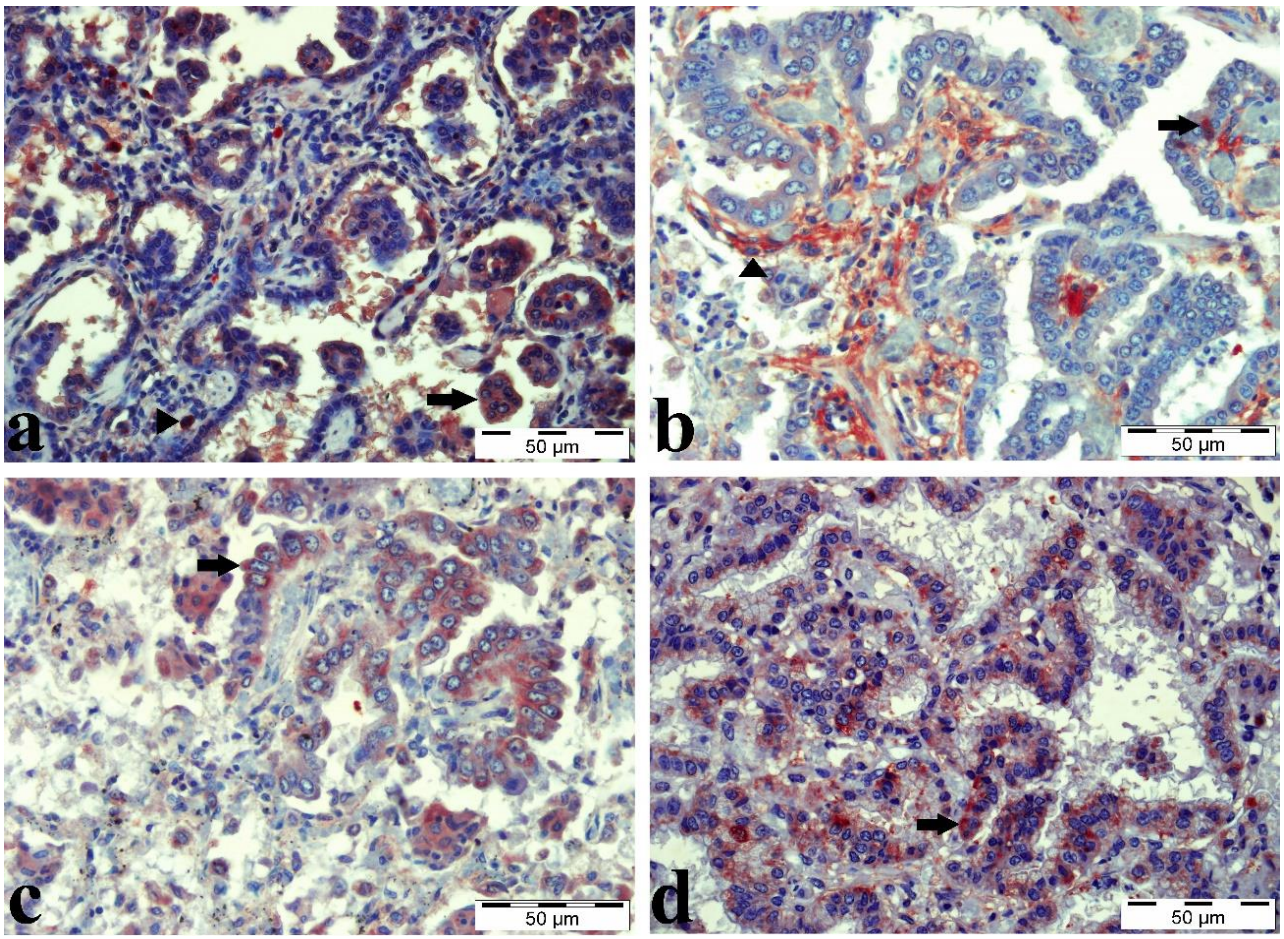

Figure 2. Lung, IHC, AEC, **a:** IL-1β immunopositive reactions in acinar structures (arrow) and lymphocytes in tumor stroma (arrowhead), **b:** IL-6 immune positive reactions in the cytoplasm of neoplastic cells forming papillary extensions (arrow) and tumor stroma (arrowhead), **c:** Intracytoplasmic IL-10 expressions in papillary structures (arrow) inside alveolar lumens **d:** IL-12β immunoreactivity in the cytoplasm of finger-like proliferations (arrowhead) in tumoral foci.

Immunohistochemical Findings

Immune positivity scores of all groups are shown in Table 1. The control group was negative for IL-1β, IL-6, IL-10 and IL-12β immunoreactivity. IL 1β-6-10 and 12β expressions were statistically increased in the Jaagsiekte group compared to the control group. In the Jaagsiekte group, IL-1β, IL-6, IL-10 and IL-12β expressions were mostly detected in the cytoplasm of cuboidal-columnar tumoral cells with acinar or papillary growths. Immune positive reactions were also observed in alveolar macrophages localized around tumoral foci.

Table 1. Immunpositivity scores of all groups

Groups	IL-1β	IL-6	IL-10	IL-12β
Control n=6	0.00±0.00[a]	0.00±0.00[a]	0.00±0.00[a]	0.00±0.00[a]
Jaagsiekte n=20	2.18±0.18[b]	2.25±0.16[b]	1.36±0.15[b]	2.45±0.16[b]
p value	<0.001	<0.001	<0.001	<0.001

[a-b] represents the statistical difference between the groups ($p<0.05$).

In addition, there was positive interleukin staining in the tumoral stroma, especially in lymphocytes and connective tissue cells. IL 1β, 6 and 12β immunoreactivities were detected especially in areas where the inflammatory reaction was severe. On the other hand, IL-10 positive staining was more pronounced in areas where the severity of the inflammatory reaction decreased (Figure 2).

DISCUSSION

IL-1β, a pro-inflammatory interleukin, synthesized by macrophages acts as an alarm cytokine and regulates chronic inflammation (Bhat et al., 2014; Li et al., 2020). IL-1β is involved in many stages of malignant processes such as initiation and promotion of carcinogenesis; tumor development, metastasis and invasion and is correlated with tumor progression in patients with NSCLC in many studies (Tekpli et al., 2013; Li et al., 2020; Ding et al., 2021). Petrella et al., (2012) noted that IL-1β is an important pro-invasive factor in NSCLCs. Kim et al., (2013) emphasized that IL-1β is an important prognostic marker for patients with advanced NSCLC. Bhat et al., (2014) determined that the polymorphism in the Il-1β gene was significantly associated with an increased risk of NSCLC. In a similar study, Ding et al. (2020) reported that IL-1β was associated with poor long-term prognosis in early lung adenocarcinoma patients. In another study, Li et al. (2020) found that both the incidence of lung cancer and mortality rates were significantly reduced by inhibition of IL-1β. There are very few studies evaluating various interleukin levels in OPA, which is an important chronic respiratory disease of sheep (Larruskain et al., 2012; Larruskain et al., 2015; Karagianni et al., 2019). As a result of their RNA-Seq analysis, Karagianni et al. (2019) revealed that IL-1β expression did not change significantly between experimentally infected sheep and normal sheep. In the current study, it was determined that IL-1β expression in naturally infected sheep with JSRV was statistically increased compared to healthy control group sheep. IL-1β immunoreactivity was higher in the Jaagsiekte group. It was interpreted that IL-1β, which increased in correlation with the severity of inflammation similar to the literature data in human medicine (Petrella et al., 2012; Kim et al., 2013; Tekpli et al., 2013; Bhat et al., 2014; Li et al. 2020; Ding et al., 2021), may contribute to the progression of Jaagsiekte on the basis of chronic inflammation.

The high serum concentration of IL-6, an important tumor-enhancing cytokine, is associated with tumor stage, size, metastasis, and poor survival in many types of human cancer, including NSCLC (Islas-Vazquez et al., 2020; Ke et al., 2020; Su et al., 2020). In veterinary medicine, there is only one study evaluating IL-6 levels in OPA, and in that study, IL-6 was upregulated in the experimentally infected group compared to the control group (Karagianni et al., 2019). Islas-Vazquez et al. (2020) found that human lung cancers had very high levels of IL-6 compared to healthy subjects. They reported that the level of this cytokine decreased in the group with a high overall survival rate after treatment. Dutkowska et al., (2021) observed increased expression of IL-6 in both tumoral and tumor-adjacent tissue of patients with NSCLC. They interpreted this increase can promote inflammatory processes in lung carcinogenesis. Pan et al., (2020) demonstrated that IL-6 increased the epithelial-mesenchymal transition, which plays a vital role in tumor invasion in lung adenocarcinoma cells. Su et al., (2020) suggested that IL-6 is an important therapeutic target for NSCLC metastasis and a highly promising prognostic marker for the disease. Kiss et al. (2020) reported that IL-6 increased cellular migration and proliferation in lung adenocarcinomas. In the current study, IL-6 expression was significantly increased in the OPA group compared to the control group, as

previously reported by Karagianni et al. (2019). Parallel to the IL-1β results, IL-6 immunopositivity was higher in the Jaagsiekte group. This suggested that, similar to the results of different researchers in human medicine (Islas-Vazquez et al., 2020; Ke et al., 2020; Su et al., 2020; Dutkowska et al., 2021), IL-6 may be a remarkable marker in lung cancers of animals, especially Jaagsiekte, as it is in humans. The results obtained from this study led to the conclusion that the inflammatory process in the tumor microenvironment may play a role in the development of Jaagsiekte.

IL-10, an important anti-inflammatory cytokine, regulates autoimmunity, cellular proliferation, survival, apoptosis and angiogenesis (Vahl et al., 2017). IL-10 is mostly produced by tumor-associated macrophages (TAMs, M2 macrophages) in the tumor microenvironment, as well as by CD4, Tregs or CD8 T cells and even tumor cells themselves (Pang et al., 2017). In particular, TAMs increase tumor growth and angiogenesis by releasing various cytokines and promote tumor invasion and metastasis by degrading the extracellular matrix (ECM) (Yang et al., 2019; Hu et al., 2020). The clinical effect of IL-10 in cancers is not fully understood (Hsu et al., 2016). Patients with NSCLC expressing high levels of IL-10 have a poor prognosis. Conversely, high levels of IL-10 produced by tumor-infiltrating CD8+ cells indicate a favorable prognosis (Gao et al., 2020). Larruskain et al. (2015) determined that there was a polymorphism in the IL-10 gene in sheep with OPA. Parallel to IL-1β results, Karagianni et al. (2019) revealed that IL-10 expression did not change significantly between experimentally induced OPA infection sheep and normal sheep. Similar to previously reported (Pang et al., 2017; Vahl et al., 2017), IL-10 expressions in this study were mostly observed in tumor-associated macrophages and tumor cells themselves. Contrary to Karagianni et al. (2019), in the current study, IL-10 expression was significantly increased in the Jaagsiekte group compared to the control group, the increase was particularly much higher in areas with less inflammatory reaction. These findings also supported the anti-inflammatory properties of IL-10 (Vahl et al., 2017).

IL-12 is mostly produced by monocytes, macrophages, and other antigen-presenting cells, and it activates NK cells by targeting them (Arango Duque and Descoteaux, 2014; Turner et al., 2014). IL-12, which is an important regulator of the immune response, has various anti-tumoral effects (Airoldi et al., 2009; D'Amico et al., 2012). IL-12 is a useful predictive and prognostic marker for patients with lung adenocarcinoma (Bugalho et al., 2016). Larruskain et al. (2012) found that the IL-12 microsatellite was the least polymorphic with 7 alleles in OPA. In another study, Larruskain et al. (2015) reported that, together with IL-2 and IL-4, IL-10 is one of the important interleukin genes involved in OPA. Similar to the results of IL-1β and IL-6 immunoreactivities in this study, IL-12β showed a significant increase in the OPA groups compared to the control group, in parallel with the severity of the inflammation.

CONCLUSION

In conclusion, it was determined that various interleukins were produced from tumoral cells and tumor microenvironment elements, especially TAMs, and these interleukins showed pro-inflammatory effects, except for IL-10. More detailed analyzes are essential to determine whether these interleukins have a direct effect on the progression of Jaagsiekte.

ACKNOWLEDGMENTS

Conflict of Interests: The authors declared that there is no conflict of interests.

Financial Disclosure: The authors declared that this study has received no financial support.

Author's Contributions: *EKa designed the study. HN, AY and EKu performed histopathological and immunohistochemical staining. EB and SD analyzed the immunohistochemical and histopathological results. EKa: Emin Karakurt, EB: Enver Beytut, SD: Serpil Dağ, HN: Hilmi Nuhoğlu, AY: Ayfer Yildiz, EKu: Emre Kurtbaş*

REFERENCES

Airoldi I, Di Carlo E, Cocco C, *et al.* IL-12 can Target Human Lung Adenocarcinoma Cells and Normal Bronchial Epithelial Cells Surrounding Tumor Lesions. PLoS One. 2009; 4(7):e6119.

Arango Duque G, Descoteaux A. Macrophage cytokines: involvement in immunity and infectious Diseases. Front Immunol. 2014; 5:491.

Belalmi NEH, Sid N, Bennoune O, Ouhida S, Heras ML, Leroux C. Evidence of Jaagsiekte Sheep Retrovirus-induced pulmonary adenocarcinoma in Ouled Djellal Breed Sheep in Algeria. Vet Res Forum. 2020; 11(1):93-95.

Bhat IA, Naykoo NA, Qasim I, *et al.* Association of interleukin 1 Beta (IL-1β) polymorphism with mRNA expression and risk of non small cell lung cancer. Meta Gene. 2014; 2:123-133.

Bugalho A, Martins C, Silva Z, *et al.* Immature myeloid cells and tolerogenic cytokine profile in lung adenocarcinoma metastatic lymph nodes assessed by endobronchial ultrasound. Tumour Biol. 2016; 37(1):953-961.

Ding X, Zhang J, Shi M, *et al.* High expression level of interleukin-1β is correlated with poor prognosis and PD-1 expression in patients with lung adenocarcinoma. Clin Transl Oncol. 2021; 23(1):35-42.

Dutkowska A, Szmyd B, Kaszkowiak M, Domańska-Senderowska D, Pastuszak-Lewandoska D, Brzeziańska-Lasota E, *et al.* Expression of inflammatory interleukins and selected mRNAs in non-small cell lung cancer. Sci Rep. 2021; 11(1):5092.

D'Amico L, Ruffini E, Ferracini R, Roato I. Low dose of IL-12 stimulates T cell response in cultures of PBMCs derived from non small cell lung cancer patients. J Cancer Ther. 2012; 3(4):337-342.

Gao Y, Lu J, Zeng C, *et al.* IL-10 suppresses IFN-γ-mediated signaling in lung adenocarcinoma. Clin Exp Med. 2020; 20(3): 449-459.

Gomes M, Archer F, Girard N, *et al.* Blocked expression of key genes of the angiogenic pathway in JSRV-induced pulmonary adenocarcinomas. Vet Res. 2017; 48(1):76.

Hsu TI, Wang YC, Hung CY, *et al.* Positive feedback regulation between IL10 and EGFR promotes lung cancer formation. Oncotarget. 2016; 7(15):20840-20854.

Hu X, Gu Y, Zhao S, Hua S, Jiang Y. Increased IL-10+CD206+CD14+M2-like macrophages in alveolarlavage fluid of patients with small cell lung cancer. Cancer Immunol Immunother. 2020; 69(12):2547-2560.

Islas-Vazquez L, Aguilar-Cazares D, Galicia-Velasco M, *et al.* IL-6, NLR, and SII markers and their relation with alterations in CD8+ T-Lymphocyte subpopulations in patients treated for lung adenocarcinoma. Biology (Basel). 2020; 9(11):376.

Karagianni AE, Vasoya D, Finlayson J, Martineau HM, Wood AR, Cousens C, *et al.* Transcriptional response of ovine lung to infection with Jaagsiekte Sheep Retrovirus. J Virol. 2019; 93(21):e00876-19.

Ke W, Zhang L, Dai Y. The role of IL-6 in immunotherapy of non-small cell lung cancer (NSCLC) with immune-related adverse events (irAEs). Thorac Cancer 2020; 11(4):835-839.

Kim JW, Koh Y, Kim DW, *et al.* Clinical implications of VEGF, TGF-β1, and IL-1β in patients with advanced non-small cell Lung cancer. Cancer Res Treat. 2013; 45(4):325-333.

Kiss E, Abdelwahab EHMM, Steib A, *et al.* Cisplatin treatment induced interleukin 6 and 8 Production alters lung adenocarcinoma cell migration in an oncogenic mutation dependent manner. Respir Res. 2020; 21(1):120.

Larruskain A, Esparza-Baquer A, Minguijón E, Juste RA, Jugo BM. SNPs in candidate genes MX Dynamin-like GTPase and Chemokine (C-C motif) receptor-5 are associated with ovine pulmonary adenocarcinoma progression in Latxa Sheep. Anim Genet 2015; 46 (6):666-675.

Larruskain A, Jugo BM. Retroviral infections in sheep and goats: Small Ruminant Lentiviruses and host interaction. Viruses. 2013; 5(8):2043-2061.

Larruskain A, Minguijón E, Arostegui I, Moreno B, Juste RA, Jugo BM. Microsatellites in immune-relevant regions and their associations with Maedi-Visna and ovine pulmonary adenocarcinoma viral diseases. Vet Immunol Immunopathol. 2012; 145(1-2):438-446.

Lee AM, Wolfe A, Cassidy JP, *et al.* First confirmation by PCR of Jaagsiekte Sheep Retrovirus in Ireland and prevalence of ovine pulmonary adenocarcinoma in adult sheep at Slaughter. Ir Vet J. 2017; 70:33.

Li L, Li D, Chen Y. miRNA-26a Blocks Interleukin-2-mediated migration and proliferation of non-small cell lung cancer cells via vascular cell adhesion molecule-1. Transl Cancer Res. 2020; 9 (3):1768-1778.

Li R, Ong SL, Tran LM, *et al.* Author Correction: Chronic IL-1β-induced inflammation regulates epithelial-to-mesenchymal transition memory phenotypes via epigenetic modifications in non-small cell lung cancer. Sci Rep. 2020; 10(1):4386. Erratum for: Sci Rep. 2020; 10(1):377.

Pan T, Zhang F, Li F, *et al.* Shikonin blocks human lung adenocarcinoma cell migration andinvasion in the inflammatory microenvironment via the IL-6/STAT3 Signaling Pathway. Oncol Rep. 2020; 44(3):1049-1063.

Pang L, Han S, Jiao Y, Jiang S, He X, Li P. Bu Fei decoction attenuates the tumor associated macrophage stimulated proliferation, migration, invasion and immunosuppression of non-small cell lung cancer,partially via IL-10 and PD-L1 Regulation. Int J Oncol. 2017; 51(1):25-38.

Petrella BL, Armstrong DA, Vincenti MP. Interleukin-1 Beta and transforming growth factor-beta 3 cooperate to activate matrix metalloproteinase expression and invasiveness in A549 lung adenocarcinoma Cells. Cancer Letters. 2012; 325(2):220-226.

Scott PR, Dagleish MP, Cousens C. Development of superficial lung lesions monitored on farm by serial ultrasonographic examination in sheep with lesions confirmed as ovine pulmonary adenocarcinoma at Necropsy. Ir Vet J. 2018; 71:23.

Su XH, Zhu YR, Hou YJ, Li K, Dong NH. PVT1 Induces NSCLC cell migration and invasion by regulating IL-6 via Sponging miR-760. Mo CelProbes. 2020; 54:101652.

Tekpli X, Landvik NE, Anmarkud KH, Skaug V, Haugen A, Zienolddiny S. DNA Methylation at promoter regions of interleukin 1B, interleukin 6, and interleukin 8 in non-small cell lung Cancer. Cancer Immunol Immunother. 20131; 62(2):337-345.

Toma C, Bâlteanu VA, Tripon S, *et al.* Exogenous Jaagsiekte Sheep Retrovirus Type 2 (exJSRV2) Related to ovine pulmonary adenocarcinoma (OPA) in Romania: Prevalence, anatomical forms, pathological description, immunophenotyping and virus identification. BMC Vet Res. 2020; 16(1):296.

Turner MD, Nedjai B, Hurst T, Pennington DJ. Cytokines and chemokines: At the crossroads of cell signalling and inflammatory disease. Biochim Biophys Acta. 2014; 1843(11):2563-2582.

Vahl JM, Friedrich J, Mittler S, *et al.* Interleukin-10-Regulated tumour tolerance in non-small cell lung cancer. Br J Cancer. 2017; 117(11):1644-1655.

Yang L, Dong Y, Li Y, *et al.* IL-10 derived from M2 macrophage promotes cancer stemness via JAK1/STAT1/NF-κB/Notch1 pathway in non-small cell lung cancer. Int J Cancer. 2019; 145(4):1099-1110.

Yue T, Zheng X, Dou Y, *et al.* Interleukin 12 shows a better curative effect on lung cancer than paclitaxel and cisplatin doublet chemotherapy. BMC Cancer. 2016; 16(1):665.

Original Article https://doi.org/10.47748/tjvr.1069768

TJVR 2022; 6 (1): 15-18

Turkish Journal of Veterinary Research

https://dergipark.org.tr/tr/pub/tjvr

e-ISSN: 2602-3695

Monitoring of oxidative stress and TNF-α status during the healing process in hair goats with metritis

Serdal Kurt [1] Funda Eşki [2] Leyla Mis [3]

[1] *Department of Veterinary, Elbistan Vocational School, Kahramanmaraş Istiklal University, Kahramanmaraş, Turkey*
[2] *Department of Obstetrics and Gynecology, Faculty of Veterinary Medicine, Cukurova University, Adana, Turkey*
[3] *Department of Physiology, Faculty of Veterinary Medicine, Van Yuzuncu Yil University, Van, Turkey*

Correspondence: *Funda Eşki (feski@cu.edu.tr)*

Received: 08.02.2022 Accepted: 08.03.2022

ABSTRACT

Objective: This study aimed to monitor oxidative stress parameters including total antioxidant status (TAS) and total oxidant status (TOS), and tumor necrosis factor-alpha (TNF-α) level during the healing process in hair goats with metritis.

Materials and Methods: This study was carried out on a total of 25 hair goats with metritis (n=10; Group 1) and healthy (n=15; Group 2). The beginning of the study was accepted as day 0. In both Group 1 and Group 2, blood samples were collected on days 0 (first measurement day), 14 (second measurement day) and 28 (third measurement day) of the study for TAS, TOS and TNF-α analyzes. In addition, oxidative stress index (OSI) was calculated using TAS and TOS values.

Results: It was found that TAS level decreased in Group 1 compared to Group 2 at the first measurement day ($p<0.05$). However, TOS, OSI and TNF-α levels increased in Group 1 compared to Group 2 ($p<0.01$). At the second measurement day, TOS and OSI values were higher in Group 1 than Group 2 ($p<0.05$).

Conclusion: In conclusion, the antioxidant system weakened, oxidative stress and TNF-α levels increased in animals with metritis compared to healthy animals. However, at the third measurement time, all parameters became similar between groups.

Keywords: *Hair goat, Metritis, Oxidative stress, TNF-α*

INTRODUCTION

Metritis is defined as inflammation of the uterus (Kurt et al., 2019). It is known that the most important causes of metritis are uterine contamination resulting from dystocia or placental retention (Majeed, 1994). It is among the main reproductive disorders in goats (Kulsum et al., 2020) and is considered the major cause of infertility (Majeed, 1994). This reproductive disorder is responsible for decreased milk yield and increased culling rate and therefore reduced profitability in goat herds (Sayeed et al., 2020). It has an incidence of 23.4% (Kulsum et al., 2020) and a prevalence of 4.5% (Sayeed et al., 2020). The disease is well recognized with clinical findings such as fever and fetid watery red-brown uterine discharge. It is associated with immune dysfunction in the postpartum period (Kurt et al., 2019). On the other hand, there is a relationship between the inflammation and oxidative stress (Celi, 2010), and is closely linked to the occurrence of metritis (Mikulková et al., 2020), as well as many diseases (Lykkesfeldt and Svendsen, 2007). Oxidative stress occurs when the antioxidant defense capacity is exceeded by the production of ROS in the body (Lykkesfeldt and Svendsen, 2007; Sordillo and Aitken, 2009; Kurt et al., 2021).

Oxidative stress can cause oxidative damage to components of cells such as DNA, lipids and proteins (Lykkesfeldt and Svendsen, 2007; Cecchini et al., 2018), can result in cell death by apoptosis and necrosis or structural tissue damage. Therefore, it can increase susceptibility to diseases (Lykkesfeldt and Svendsen, 2007). Oxidative stress may be associated with uterine infections in the periparturient period (Yazlık et al., 2019; Mikulková et al., 2020). On the other hand, it is known that cytokines such as TNF-α are closely linked to the inflammation caused by the infection. Moreover, TNF has several roles in reproductive function, and it is involved in many biological events such as stimulation of cell proliferation and differentiation, induction of cell apoptosis (Skarzynski et al., 2009). It is also stated that the level of TNF-α increases in animals that experience uterine infection (Williams et al., 2008). For the reasons mentioned above, it is thought that both oxidative stress and TNF levels may differ in animals with uterine infection. It is also estimated that there may be differences in the level of those parameters during the healing process. Therefore, the present study aimed to monitor oxidative stress parameters including total antioxidant status (TAS) and total oxidant status (TOS), and tumor necrosis factor-alpha (TNF-α) level during the healing process in hair goats with metritis.

MATERIALS and METHODS

Ethical approval

This study was approved by the Ethics Committee of Ceyhan Veterinary Faculty, Cukurova University, Adana, Turkey (approval number: 01/01 and 24.01.2022).

Animals and study design

This study was carried out on a total of 25 hair goats with healthy (n=15) and metritis (n=10). All goats had similar age, body condition score and parity, and they were within the first two weeks postpartum at the start of the study. The goats were subjected to clinical examination including vaginal examination before the study. Metritis was characterized by fetid watery red brown uterine discharge, high fever and systemic signs of diseases (Sheldon et al., 2006). Animals with high fever, odorous watery red-brown vaginal discharge were defined as metritis. Animals that did not show any signs of disease as a result of clinical examination were considered healthy. The goats with metritis and healthy were recorded in Group 1 and Group 2, respectively. Goats with metritis were used systemic broad-spectrum antibiotics and fluid therapy according to farm's routine treatment protocol, and corticosteroids were also given when necessary. Animals that did not recover from the disease during the study were not included in the study. The beginning of the study was accepted as day 0. In both Group 1 and Group 2, blood samples were collected from the jugular vein into sterile serum tubes with clot activator on days 0 (first measurement day), 14 (second measurement day) and 28 (third measurement day) of the study. All blood samples were centrifuged at 1500 x g for 10 min, then serum samples were collected and stored at -20°C until analysis.

Laboratory analysis

Determination of TAS, TOS and TNF-α levels

Serum TAS and TOS levels were measured with the Enzyme Linked Immunosorbent Assay (ELISA) devive (Stat Fax-2100, Awareness®, USA) using commercial kits (Rel Assay Diagnostics®, Turkey). Serum TNF-α level was measured using an ELISA device (Stat Fax-2100, Awareness®, USA) and commercial kit (TNF-α ELISA kits, Bt Lab®, China). Oxidative stress index (OSI) calculated as previously defined (Kurt et al., 2021).

Statistical analysis

Statistical analyzes were performed using the SPSS package program. The obtained data were analyzed statistically according to the non-parametric Mann-Whitney U test. All results were presented as mean ± standard deviation (mean ± SD) and $p<0.05$ was considered significant.

RESULTS

It was determined that the TAS level decreased in Group 1 compared to Group 2 at the first measurement day ($p<0.05$). However, other parameters within TOS, OSI and TNF-α significantly increased in Group 1 compared to Group 2 ($p<0.01$). On the second measurement day, TOS and OSI values were higher in Group 1 than Group 2 ($p<0.05$), but there was no difference between groups in terms of TAS and TNF-α values ($p>0.05$). At the time of the third measurement, it was found that TAS, TOS, OSI, and TNF-α levels were similar between Group 1 and Group 2 ($p>0.05$). TAS, TOS, OSI, and TNF-α results obtained in the two groups are presented in detail in Table 1.

Table 1. TAS, TOS, OSI and TNF-α results measured in Group 1 and Group 2.

Parameters	Groups	First measurement (Mean ± SD)	Second measurement (Mean ± SD)	Third measurement (Mean ± SD)
TAS (mmol/L)	Group 1	1.29±0.64^{a}	1.42±0.44	1.38±0.23
	Group 2	1.80±0.42^{b}	1.44±0.26	1.36±0.26
TOS (umol/L)	Group 1	10.08±4.20^{a*}	6.33±2.07^{a}	5.66±0.78
	Group 2	5.26±1.09^{b*}	5.05±0.58^{b}	5.03±1.28
OSI	Group 1	0.97±0.53^{a*}	0.49±0.21^{a}	0.43±0.12
	Group 2	0.31±0.10^{b*}	0.36±0.07^{b}	0.39±0.14
TNF-α (ng/L)	Group 1	1.63±0.24^{a*}	0.93±0.29	0.89±0.31
	Group 2	1.01±0.17^{b*}	0.96±0.29	0.91±0.29

Different letters in the same column represent statistical difference for similar parameters ($p<0.05$). *$p<0.01$ TAS: Total antioxidant status, TOS: Total oxidant status, OSI: Oxidative stress index, TNF-α: tumor necrosis factor-alpha.

DISCUSSION

The presented study investigated oxidative stress parameters including TAS, TOS and OSI, and TNF-α level during the healing process in Hair goats with metritis. In addition, a healthy group was formed to compare these results with healthy animals.

Metritis is known as an important cause of infertility (Majeed, 1994). Furthermore, various gynecological disorders, including metritis, are vital factors that cause economic losses in small ruminant breeding (Kulsum et al., 2020). Metritis can occur under the influence of many bacterial contaminations (Mikulková et al., 2020; Doumtsop et al., 2021), and can cause inflammation, leukocyte infiltration, edema and myometric degenerations in all layers of the uterine wall (Mikulková et al., 2020), and thus leads to fertility problems in many ways. Sheldon et al. (2006) stated that the occurrence of metritis is usually associated with deficiencies in the immune system in dairy cows. On the other hand, it has been informed that oxidative stress may predispose factor to metritis (Mikulková et al., 2020). Huang et al. (2021) reported that ROS production increased in goats during periparturient period due to metabolic adaptation process and catabolic energy metabolism due to energy deficit in this period. Therefore, it is known that this period is quite critical in terms of diseases and oxidative stress. Similarly, Mikulková et al. (2020) reported that oxidative stress was higher in cows with metritis during the early postpartum period. The oxidative stress findings of the presented study support this information. It was observed that oxidative stress increased on the day the disease was diagnosed (first measurement day) in goats with metritis. The reason for this situation was thought to be the weak antioxidant defense system, because TAS level was significantly lower in animals with metritis compared to healthy animals. In addition, in this study, it was revealed that the antioxidant level of the animals increased in parallel with the recovery from the disease. On the second measurement day, the animals recovered in general, but the oxidative stress level was still higher in Group 1 than in Group 2, although the antioxidant level returned to normal. No signs of diseases were observed in any animal on the third measurement day. In addition, there was no difference between Group 1 and Group 2 in terms of oxidative stress parameters in this period. This situation reveals the relationship between metritis and oxidative stress in goats. However, we think that oxidative stress level should be determined before metritis occurs. Thus, it can be revealed whether it can be used in the early diagnosis of the disease. However, in the presented study, differences in oxidative stress and TNF-α levels were observed only during the healing process. TNF-α is known as a cytokine associated with the inflammatory syste (Skarzynski et al., 2009; Kushibiki, 2011). Moreover, TNF-α has various immune system functions, including antimicrobial activity and mediation of inflammation (Kushibiki, 2011). Williams et al. (2008) stated that the level of TNF-α increased in animals with uterine infection. So, considering role of TNF-α in the inflammatory system, its level was investigated in goats with metritis. In the presented study, TNF-α level increased significantly on the first measurement

day in Group 1 compared to Group 2. We think that this is due to the activation of the inflammatory system due to metritis. This assumption is confirmed by the TNF-α level on the second and third measurement days. So, TNF-α level of Group 1 became similar to Group 2 in parallel with the recover of the disease. However, we think that TNF level should be investigated more comprehensively in animals with uterine infection and it should be determined whether it can be used in the early diagnosis of the metritis in goats.

CONCLUSION

This study investigated the changes in oxidative stress parameters and TNF-α levels during the healing process in hair goats with metritis. On the first day of measurement, the antioxidant system weakened, oxidative stress and TNF-α levels increased in animals with metritis compared to healthy animals. Similarly, oxidative stress was still high in animals with metritis at the second measurement time. On the other hand, at the third measurement time, all parameters became similar between groups. However, we think that this situation should be investigated comprehensively by including treatment protocols and pathogen species that cause metritis in future studies.

ACKNOWLEDGMENTS

Conflict of Interests: The authors declared that there is no conflict of interests.

Financial Disclosure: The authors declared that this study has received no financial support.

Author's Contributions: SK and FE contributed to the study conception and design. LM contribution to laboratory work. Supervision/Consultancy (SK and FE), Data collecting (FE and SK), Literature research (SK and FE), Writing the article (SK and FE), Critical review (FE and SK). All authors read and approved the final manuscript. SK: Serdal KURT, FE: Funda EŞKİ, LM: Leyla MİS

REFERENCES

Cecchini S, Piccione G, Saoca C, Giangrosso G, Caputo AR, Fazio F. Redox status, lipid peroxidation and protein oxidation levels in small ruminants. J Anim Feed Sci. 2018; 27(1):81-85.

Celi P. The role of oxidative stress in small ruminants' health and production. Rev Bras de Zootec. 2010; 39:348-363.

Doumtsop CLM, Kouamo J, Njintang NY, Tangwa BV, Amatama LMM, Zangue CT. Prevalence, etiology and risk factors associated with chronic metritis in small ruminants in Adamawa Region (Cameroon). J Infertil Reprod Biol. 2021; 9(4):147-154.

Huang Y, Wen J, Kong Y, *et al.* Oxidative status in dairy goats: periparturient variation and changes in subclinical hyperketonemia and hypocalcemia. BMC Vet Res. 2021; 17:238.

Kulsum U, Juli MSB, Zohara BF, Islam MN, Akther M. Incidence of reproductive disorders of goat in Dinajpur district of Bangladesh. Asian J Med Biol Res. 2020; 6(2):212-221.

Kurt S, Salar S, Salar MÖ. Antibiogram and pathogen isolation from vaginal discharge in dairy cows with metritis. Vet Hekim Der Derg. 2019; 90(2):66-70.

Kurt S, Eşki F, Mis L, Demir PA. Evaluation of oxidative stress, immune system and mineral concentrations in milk and serum of cows with clinical and subclinical mastitis naturally infected by *Staphylococcus aureus*. Kafkas Univ Vet Fak Derg. 2021; 27(6):755-762.

Kushibiki S. Tumor necrosis factor-α induced inflammatory responses in cattle. Anim Sci J. 2011; 82(4):504-511.

Lykkesfeldt J, Svendsen O. Oxidants and antioxidants in disease: oxidative stress in farm animals. Vet J. 2007; 173(3):502-511.

Majeed AF. Obstetrical problems and their management in Iraqi goats. Small Rumin Res. 1994; 14(1):73-78.

Mikulková K, Kadek R, Filípe J, Illek J. Evaluation of oxidant/antioxidant status, metabolic profile and milk production in cows with metritis. Ir Vet J. 2020; 73:1-11.

Sayeed MA, Khatun MS, Bari MS, Dash AK, Haldar PK, Sarker BK. Prevalence of gynecological disorders of goat and pattern of drug used at Chuadanga, Bangladesh. Agric Sci Digest. 2020; 40(4):424-429.

Sheldon IM, Lewis GS, LeBlanc S, Gilbert RO. Defining postpartum uterine disease in cattle. Theriogenology, 2006; 65(8):1516-1530.

Sordillo LM, Aitken SL. Impact of oxidative stress on the health and immune function of dairy cattle. Vet Immunol Immunopathol. 2009; 128(1-3):104-109.

Skarzynski DJ, Piotrowska KK, Bah MM *et al.* Effects of exogenous tumour necrosis factor-α on the secretory function of the bovine reproductive tract depend on tumour necrosis factor-α concentrations. Reprod Domest Anim. 2009; 44(3):371-379.

Williams EJ, Sibley K, Miller AN, *et al.* The effect of *Escherichia coli* lipopolysaccharide and tumour necrosis factor alpha on ovarian function. Am J Reprod Immunol. 2008; 60(5):462-473.

Yazlık MO, Çolakoğlu HE, Pekcan M *et al.* The evaluation of superoxide dismutase activity, neutrophil function, and metabolic profile in cows with retained placenta. Theriogenology, 2019; 128:40-46.

Original Article https://doi.org/10.47748/tjvr.1055929

TJVR 2022; 6 (1): 19-26

Turkish Journal of Veterinary Research

https://dergipark.org.tr/tr/pub/tjvr

e-ISSN: 2602-3695

A Macroanatomical study on coronary veins in Southern Karaman Sheep

Hülya Kara[1] Zekeriya Özüdoğru[2]

[1] *Department of Anatomy, Faculty of Veterinary Medicine, Atatürk University, Erzurum, Turkey*
[2] *Department of Anatomy, Faculty of Veterinary Medicine, Aksaray University, Aksaray, Turkey*

Correspondence: *Hülya Kara (h.goktas@atauni.edu.tr)*

Received: 10.01.2022 Accepted: 11.03.2022

ABSTRACT

Objective: This study aimed to reveal the coronary veins and the branches that join it to provide venous drainage of the heart in Southern Karaman sheep.

Material-Method: Eight Southern Karaman sheep's heart tissues were used in the study. Latex injection techniques were used to determine the coronary veins and the branches that join it for providing venous drainage of the heart.

Result: In the study, vena cordis magna, vena cordis media, and vv. cordis dextra was observed as venous drainage providing vessels. The vena cordis magna began in the lower third of the sulcus interventricularis paraconalis, called vena interventricularis paraconalis. This vein reached the sulcus coronarius and continued as vena circumflexus sinister. Vena cordis media was named as vena interventricularis subsinosus in sulcus interventricularis subsinosus. The vv. cordis dextra was responsible for the venous drainage of the facies atrialis of the heart.

Conclusion: In the evaluation of the study findings, it was determined that the coronary veins and the branches joined it of Southern Karaman sheep were mainly similar to other sheep breeds in the literature. Still, there were some anatomical differences, for example; vena distalis ventriculi sinistri was opening into vena circumflexus sinister, vena apicis cordis was absent, vena semicircumflexa dextri was present.

Keywords: *Anatomy, Southern Karaman sheep, Coronary vein, Latex*

INTRODUCTION

The Southern Karaman sheep breed is a different species obtained by crossing the Karagül rams bred with Akkaraman and Dağlıç sheep. This breed is one of the most preferred breeds in Turkey due to its higher yields in meat and milk production (Kaymakçı, 2008; Ertuğrul et al., 2009).

The main vessels that provide venous drainage of the heart in mammals are; vena cordis magna, vena cordis media, vv. cordis dextra and vv. cordis minimae. All of these veins end by opening into the sinus coronarius. Besides, vv. cordis minimae may open to anterior cardiac veins as well as sinus coronarius in sheep (Yadm and Gad, 1992; Yadm, 1993; Dursun, 1994; Tıpırdamaz et al., 1999; Beşoluk and Tıpırdmaz, 2001; Constantinescu, 2001).

Sinus coronarius is localized in the ventral part of the bottom parts of the truncus pulmonalis and vena cava caudalis, as a continuation of the vena azygos sinistra, and it usually opens to the vena cava caudalis as well as it may also end by opening into the atrium dextrum (Yoldaş, 2007; Aydınlık et al., 2008; Gürbüz, 2015).

The vena cordis magna is the strongest of the coronary veins and begins as the vena

interventricularis paraconalis in the distal part of the sulcus interventricularis paraconalis. By continuing within the sulcus interventricularis paraconalis, it reaches the sulcus coronarius and continues on its way as the vena circumflexus sinister and ends after opening into the sinus coronarius. During its course, vena collateralis sinister distalis, vena collateralis sinister proximalis, vena coni arteriosa join it that they drain the ventriculus sinister and septum interventriculare (Nickel et al., 1981; Evans and Christensen, 1993; Koch and Berg, 1993; Aksoy et al., 2003; Yoldaş et al., 2013; Barszcz et al., 2020).

The vena circumflexus sinister is the continuation of the vena interventricularis paraconalis and begins at the intersection of the sulcus interventricularis paraconalis and sulcus coronarius. It continues in the sulcus coronarius along the ventral edge of the auricula sinistra and terminates after opening into the sinus coronarius. During its course, vena circumflexus sinister, vena proximalis ventriculi sinistri, vena distalis ventriculi sinistri, vena marginis ventricularis sinistri accessoria, and vena marginis ventricularis sinistri join it (Gürbüz, 2015; Barszcz et al., 2020).

Vena cordis media, after originating from apex cordis as vena interventricularis subsinosus in sulcus interventricularis subsinosus, courses towards basis cordis (Aksoy et al., 2001; Aksoy et al., 2009). After draining the ventriculus dexter and atrium dextrum in facies atrialis, it usually ends by opening into the sinus coronarius and sometimes into the atrium dextrum.

During its course, vena collateralis dexter proximalis, vena collateralis dexter distalis, vena obliqua ventriculi dextri open here from the atrial surface of the ventriculus dexter. From the auricular surface, the vena collateralis sinister proximalis, vena collateralis sinister intermedia, vena collateralis sinister distalis branches and vena apicis cordis open into this vein (Aksoy et al., 2009; Kabak and Onuk, 2012; Gürbüz, 2015; Barszcz et al., 2020)

Vv. cordis dextra reaches the sulcus coronarius by providing venous drainage of the atrium dextrum and ventriculus dexter located on the right side of the heart. During the course of vv. cordis dextra, v. proximalis atrii dextri, v. coni arteriosi, v. proximalis ventriculi dextri opens into this vein (Dursun, 1994; Tıpırdamaz et al., 1999; Beşoluk and Tıpırdmaz, 2001).

The numerous and thin cordis minimae branches were mainly observed in the atrium dextrum and less frequently in the atrium sinistrum and ventriculus dexter. They collect the venous blood in the surrounding tissues and empty it into the nearest cardiac cavity (Tıpırdamaz et al., 1999).

In this study, we aimed to investigate the coronary veins that provide venous drainage of the heart in Southern Karaman sheep, an indigenous breed in Turkey.

MATERIALS and METHODS

Animal Material

The study was conducted according to ethical guidelines and under the supervision of Atatürk University Local Ethics Committee board (*Decision no: 2021-35*). Eight Southern Karaman sheep's hearts were used in the study. The Southern Karaman sheep were obtained from Konya Bahri Dağdaş International Agricultural Institute.

Method

After the sheep were anesthetized with xylazine HCl (0.3 mg/kg/IV) and ketamine HCl (2.5 mg/kg/IV), they were injected Na-Heparin (5,000 IU/mL) at a dose of 0.1 mg/kg/IV to prevent blood clotting. Then, the abdominal cavities were opened under deep anesthesia and the venous circulatory system was cleaned with 0.9% saline solution with a plastic catheter placed in the v. cava caudalis. After removing the heart, the cannulas were placed in the vena azygos sinistra to examine the coronary veins of heart. According to the previous latex injection method (Aycan and Bilge, 1984), 200 cc of latex and 10 cc of fabric dye were mixed in a beaker to disperse the dyestuff. For demonstration, the latex mixture colored with blue fabric dye was injected into the coronary veins through the cannulas placed before, and then the hearts were preserved in 10% formaldehyde solution. They were kept in 10% formaldehyde solution for 72 hours to ensure their determination. The coronary veins were dissected, and structures were identified and labeled. The terminology employed has been referenced from the Nomina Anatomica Veterinaria 6th edition (2017).

RESULTS

In this study, we observed the vena cordis magna, vena cordis media, and vv. cordis dextra. These main branches were subepicardial and partly intramyocardial. These branches terminated after transmitting the venous blood they collected, to

the sinus coronaries. Then sinus coronaries opened into vena cava caudalis (Figure 1, Figure 2a and 2b, Figure 3a and 3b, Figure 4a and 4b).

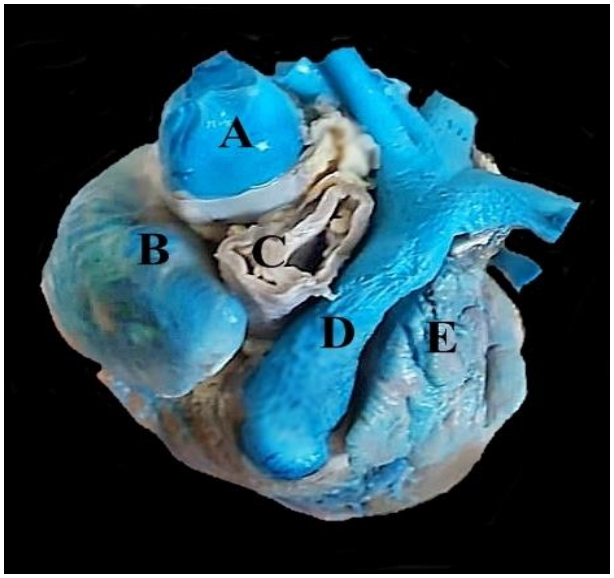

Figure 1. Dorsal view of Southern Karaman Sheep's heart;
A: vena cava caudalis, **B:** atrium dextrum, **C:** aorta, **D:** truncus pulmonalis, **E:** atrium sinistrum.

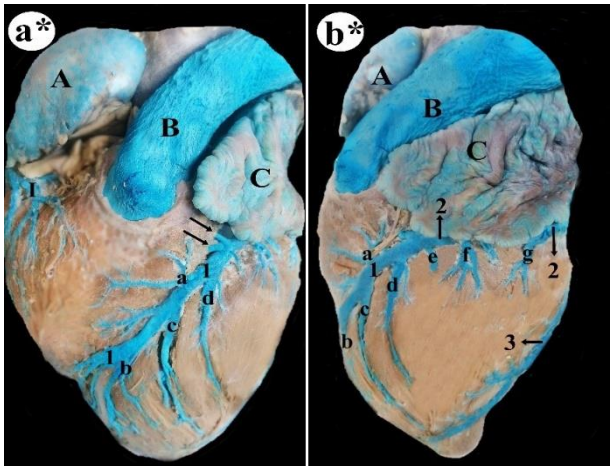

Figure 2. Vena interventricularis paraconalis and vena circumflexus sinister forming the vena cordis magna in the Southern Karaman sheep;
a*: vena interventricularis paraconalis and the branches opening into it;
A: atrium dextrum, **B:** truncus pulmonalis, **C:** atrium sinistrum, **a:** vena coni arteriosi, **b:** vena collateralis sinister distalis, **c:** vena collateralis sinister intermedia, **d:** vena collateralis sinister proximalis, **I:** the common root of vena coni arteriosi and vena proximalis ventriculi dextri, **1:** vena interventricularis paraconalis, **arrows:** septal branches.
b*: The branches opening into vena circumflexus sinister;
A: atrium dextrum, **B:** truncus pulmonalis, **C:** atrium sinistrum, **a:** vena coni arteriosi, **b:** vena collateralis sinister distalis, **c:** vena collateralis sinister intermedia, **d:** vena collateralis sinister proximalis, **e:** vena angularis, **f:** vena proximalis ventriculi sinistri, **g:** vena distalis ventriculi sinistri, **1:** vena interventricularis paraconalis, **2:** vena circumflexus sinister, **3:** vena marginis ventricularis sinistri.

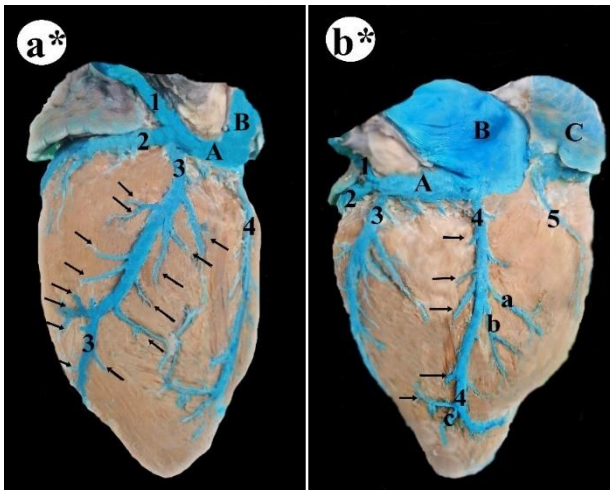

Figure 3. Sinus coronarius, vena azygos sinistra, vena marginis ventricularis sinistri and vena cordis media (vena interventricularis subsinosus) in Southern Karaman sheep;
a*: The branches opening into the vena marginis ventricularis sinistri;
A: sinus coronarius, **B:** vena cava caudalis, **1:** vena azygos sinistra **2:** vena circumflexus sinister, **3:** vena marginis ventricularis sinistri, **4:** vena cordis media (vena interventricularis subsinosus), **arrows:** the branches opening into vena marginis ventricularis sinistri over the auricular and atrial surface of ventriculus sinister.
b*: The branches opening into vena cordis media (vena interventricularis subsinosus);
A: sinus coronarius, **B:** vena cava caudalis, **C:** atrium dextrum, **a:** vena collateralis dexter proximalis, **b:** vena collateralis dexter distalis, **c:** vena apicis cordis, **1:** vena azygos sinistra **2:** vena circumflexus sinister, **3:** vena marginis ventricularis sinistri, **4:** vena cordis media (vena interventricularis subsinosus), **5:** vena distalis ventriculi dextri, **arrows:** the branches opening into vena cordis media (vena interventricularis subsinosus) from ventriculus sinister.

The sinus coronarius is the continuation of the vena azygos sinistra and is located in the sulcus coronarius at the bottom of the vena cava caudalis. It ended at the sulcus interventricularis subsinosus level by opening into the vena cava caudalis (Figure 3a and 3b). It was identified that the main branches forming the sinus coronarius by coming together were the vena cordis magna, vena cordis media, and vena marginis ventricularis sinister. It was observed that the vena azygos sinistra

progressed towards the cranial between the atrium sinistrum and the vena cava caudalis, which is the continuation of the sinus coronarius (Figure 3a and 3b).

The vena cordis magna was the most powerful vessel involved in the hearts drainage. It started in the lower 1/3 of the sulcus interventricularis paraconalis around the apex cordis, called vena interventricularis paraconalis. Upon reaching the sulcus coronarius, it continued as vena circumflexus sinister (Figure 2a and 2b). It was observed that it progressed in the caudoventral of the atrium sinistrum and ended by opening into the sinus coronarius at the margo ventricularis sinister level. During its course, branches from the atrium sinistrum and ventriculus sinister opened into it (Figure 3a and 3b).

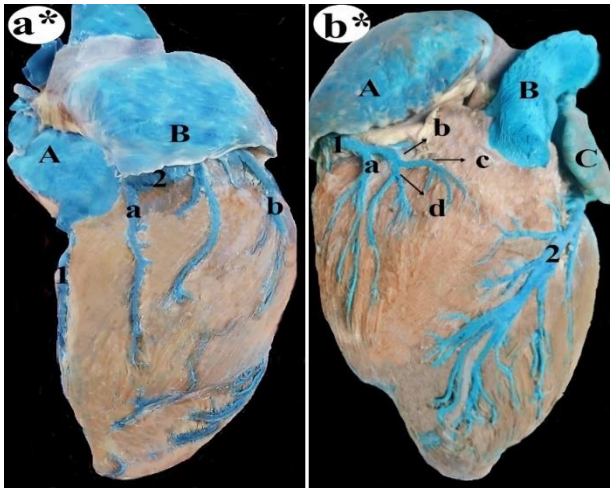

Figure 4. Vena semicircumflexa dextri formed by vv. cordis dextra in Southern Karaman sheep;

a*: The branches opening into vena semicircumflexa dextri;

A: vena cava caudalis**, B:** atrium dextrum, **a:** vena distalis ventriculi dextri, **b:** vena marginis ventricularis dextri, **1:** vena cordis media **(**vena interventricularis subsinosus), **2:** vena semicircumflexa dextri.

b*: The branches opening into vena semicircumflexa dextri;

A: atrium dextrum, **B:** truncus pulmonalis, **C:** atrium sinistrum, **a:** vena marginis ventricularis dextri, **b:** common root of vena coni arteriosi and vena proximalis ventriculi dextri, **c:** vena coni arteriosi, **d:** vena proximalis ventriculi dextri, **1:** vena semicircumflexa dextri **2:** vena interventricularis paraconalis.

The vena interventricularis paraconalis was originated on the facies auricularis of the heart, above the apex cordis, from the lower 1/3 of the sulcus interventricularis paraconalis. It moved towards the basis cordis in the cranial direction in the region close to the apex cordis after anastomosis with its thin branches with vena marginis ventricularis sinistri, vena interventricularis subsinosus, and partially vv. cordis dextra (Figure 2a). During its course, from distal to proximal, it was identified that it received vena collateralis sinister distalis, vena collateralis sinister intermedia, vena coni arteriosi, vena collateralis sinister proximalis draining ventriculus dexter, ventriculus sinister, and septum interventriculare. These main branches also received varying numbers of thin lateral branches. It was observed that the two septal branches in the proximal, close to the sulcus coronarius, were thicker than the branches draining the septum interventriculare. Collateral veins were coursed intramyocardially, obliquely, below the epicardium (Figure 2a and 2b). The branches draining the ventriculus sinister were thicker than draining the ventriculus dexter. In all studied materials, vena collateralis sinister proximalis et intermedia was stronger than vena collateralis sinister distalis. It was identified that there was a partial anastomosis between the vena collateralis sinister distalis et intermedia. and the vena marginis ventricularis sinistri's branches. The vena collateralis sinister distalis was reaching the vena interventricularis paraconalis through two main branches. It was observed that the vena coni arteriosi opened into the vena interventricularis paraconalis through two main branches between vena collateralis sinister proximalis et intermedia and oppositely with the vena collateralis sinister proximalis (Figure 2a and 2b, Figure 4b).

The vena circumflexus sinister was a continuation of the vena interventricularis paraconalis and coursed in the sulcus coronarius. Its origin was where the sulcus interventricularis paraconalis and the sulcus coronarius intersect. It coursed in the caudoventral of the atrium sinistrum, within the sulcus coronarius, and ended after opening into the sinus coronarius (Figure 3a and 3b). During its course, it receives vena proximalis atrium sinistri, vena intermedius atrium sinistri, and vena distalis atrium sinistri draining the atrium sinistrum. Furthermore, it was identified that it took branches from vena angularis, vena proximalis ventriculi sinistri, vena distalis ventriculi sinistri, and vena marginis ventricularis sinistri that drained the ventriculus sinister. It was determined that the vena angularis opened into it close to the origin of the vena circumflexus sinister. The vena proximalis ventriculi sinistri subepicardially opened into the vena circumflexus sinister, starting

as several branches with a course parallel to the margo ventricularis sinister in the facies auricularis. The vena distalis ventriculi sinistri was stronger than vena proximalis ventriculi sinistri, and the lateral branches of these two vessels made partial anastomosis. Apart from these branches, it was seen that the thin branches draining the proximal 1/3 of the ventriculus sinister were also opened into the vena circumflexus sinister (Figure 2b, Figure 3a and 3b).

The vena marginis ventricularis sinistri, the strongest of the ventricular branches, started in the apex cordis region by anastomosis with the vena interventricularis paraconalis and partially the vena interventricularis subsinosus through its thin lateral branches. It was directed towards the atrial surface from the auricular surface with an oblique course on the margo ventricularis sinister (Figure 3a and 3b). After its origin, the branches ranging from 8 to 12 from the auricular surface and 6 to10 from the atrial surface opened into it. The branches that were taken from the auricular surface were more numerous and stronger. In all of the materials studied, the vena marginis ventricularis sinistri ended by opening into the sinus coronarius. It was observed that the lateral branches taken from the atrial and auricular surfaces also anastomose with the other branches in the vicinity (Figure 2b, Figure 3a and 3b).

The vena cordis media was formed by the union of several branches above the apex cordis. It coursed from the apex cordis to the basis cordis in the sulcus interventricularis subsinosus as vena interventricularis subsinosus. It ended by opening into the sinus coronarius (Figure 3a and 3b). The first branch it taked on was the vena apicis cordis coming from the auricular surface's direction. The atrial face of ventriculus dexter was taken branches from vena collateralis dexter proximalis and vena collateralis dexter distalis from the proximal to the distal. Apart from these branches, it was determined that it received branches draining ventriculus dexter, ventriculus sinister, and septum interventriculare (Figure 3a and 3b, Figure 4a).

The vv. cordis dextra was responsible for venous drainage of the facies atrialis of the heart. Vv. cordis dextra coursed just caudoventral to the atrium dextrum (Figure 4a). During its course, it formed the semicircumflexa dextri and the vena coni arteriosi, vena proximalis ventriculi dextri, and vena marginis ventricularis dextri joined it. The branch draining the conus arteriosus area was the vena coni arteriosi, and after joining with the vena proximalis ventriculi dextri, it opened into the vena semicircumflexa dextri. The vena proximalis ventriculi dextri started in two branches from the middle 1/3 of the ventriculus dexter and progressed closely with the vena marginis ventricularis dextri. Both these veins opened into the vena semicircumflexa dextri (Figure 2a, Figure 4b). It was determined that the vena distalis ventriculi dextri originated from the lower 1/3 of the ventriculus dexter on the atrial surface and ended by opening directly into the atrium dextrum, not to the vena semicircumflexa dextri. Apart from these branches, the vv. cordis dextra also received branches that take part in venous drainage of atrium dextrum and ventriculus dexter (Figure 4a).

DISCUSSION

Coronary circulation in mammals has been studied in various vertebrates (Budras and Habel, 2003; Budras and Röck, 2009; Kupczyńska et al., 2015), such as birds (Bartyzel et al., 2009) and reptiles (Hagensen et al., 2008). Also, there are no studies on coronary veins of Southern Karaman sheep in the literature. Therefore, this study aimed to investigate the morphology of the coronary veins in Southern Karaman sheep.

Consistent with the literature (Beşoluk and Tıpırdamaz, 2001; Gürbüz, 2015; Barszcz et al., 2020; Gürbüz and Aksoy, 2020), this study determined that the main vessels providing venous drainage of the heart in Southern Karaman sheep were vena cordis magna, vena cordis media, and vv. cordis dextra.

Similar to the findings of our study, sinus coronarius was found in cattle, sheep, goat (Nickel et al., 1981), European bison (Barszcz et al., 2020), and in Tuj and Hemshin sheep (Gürbüz and Aksoy, 2020) and it drained most of the coronary veins of the heart (Genain et al., 2018). Likewise, in Hemshin sheep (Gürbüz, 2015), the sinus coronarius opened into the vena cava caudalis. Contrary to our study, it was reported that the sinus coronarius opened into the atrium dextrum (Nickel et al., 1981; Aksoy et al., 2009; Tıpırdamaz et al., 2009). Different from the study findings, Yadm and Gad (1992) reported that the sinus coronarius continued as the vena cordis magna in goats. However, in the study, similar to the literature, it was observed that the sinus coronarius was a continuation of the vena azygos sinistra (Tıpırdamaz et al., 1999; Beşoluk and

Tıpırdamaz, 2001; Aydınlık et al., 2008; Kabak and Onuk, 2012).

In Southern Karaman sheep, cattle (Budras and Habel, 2003), goats (Noor et al., 2015), Tuj sheep (Aksoy et al., 2009), Angora goats and Akkaraman sheep (Beşoluk and Tıpırdmaz, 2001), and European bison (Barszcz et al., 2020), the vena cordis magna is formed by the vena interventricularis paraconalis and vena circumflexus sinister. It ends by opening into the sinus coronarius.

In the study, unlike the findings of Barszcz et al. (2020), and Gürbüz (2015), the vena interventricularis paraconalis started from the upper side of the apex cordis. Unlike the literature findings (Beşoluk and Tıpırdamaz, 2001; Aksoy et al., 2009; Barone, 2011), we found that the vena interventricularis paraconalis anastomosed with the vena marginis ventricularis sinistri and partially with vv. cordis dextra through the lateral branches in addition to the vena media in the apex cordis region. Similar to the literature findings (Noor et al., 2015; Barszcz et al., 2020), it was determined that the branches draining the ventriculus sinister and opening into the vena interventricularis paraconalis were stronger than the branches draining the ventriculus dexter and opening into the vena interventricularis paraconalis. Unlike the findings in the literature (Aksoy et al., 2009; Kabak and Onuk, 2012; Gürbüz, 2015; Barszcz et al., 2020), this study showed that the vena collateralis sinister intermedia was as strong as the vena collateralis sinister proximalis. Similar to the literature findings (Beşoluk and Tıpıdamaz, 2001; Barszcz et al., 2020), this study identified that the vena collateralis sinister proximalis was stronger than vena collateralis sinister distalis.

Similar to the literature findings (Gürbüz, 2015; Barszcz et al., 2020; Gürbüz and Aksoy, 2020), the vena interventricularis paraconalis turned into vena circumflexus sinister in the sulcus coronarius in Southern Karaman sheep, and these two branches together shaped the v. cordis magna. Similar to Gürbüz and Aksoy's (2020) study, the vena proximalis ventriculi sinistri ended by opening into the vena circumflexus sinister. Gürbüz (2015) reported that vena marginis ventricularis sinistri in Hemshin sheep and vena angularis in two Tuj and three Hemshin sheep anastomosed with a proximal branch opening into vena interventricularis paraconalis. Unlike these findings, this study identified that the vena proximalis ventriculi sinistri made partial anastomosis with the lateral branches of the vena distalis ventriculi sinistri. It has been reported that the vena distalis ventriculi sinistri opens into the sinus coronarius in five Tuj sheep (Aksoy et al., 2009), roe deer (Kabak and Onuk, 2012), and Akkaraman sheep (Beşoluk and Tıpırdamaz, 2001). Different from these findings, the study found that the vena distalis ventriculi sinistri opened to the vena circumflexus sinister. Unlike the study's findings, Gürbüz (2015) and Aksoy et al. (2009) found that this vein did not exist.

Barszcz et al. (2020) reported that the vena marginis ventricularis sinistri started in the middle of the apex cordis or margo ventricularis sinister. As reported by Gürbüz (2015) it began in the apex cordis region of the vena marginis ventricularis sinistri. As reported by Beşoluk and Tıpırdamaz (2001), it started with anastomosis with vena interventricularis paraconalis and partly with the vena interventricularis subsinosus through its thin lateral branches. Similar to the literature findings (Beşoluk and Tıpırdamaz, 2001; Gürbüz, 2015; Barszcz et al., 2020) it was found that it ended by opening into the sinus coronarius. It has been reported that in European bison (Barszcz et al. 2020) various numbers of branches in the auricular and atrial surface join it and also, it receives 6-9 branches in the auricular surface, and 5-8 branches in the atrial surface in Tuj and Hemshin sheep (Gürbüz, 2015). In this study, it was seen that the vena marginis ventricularis sinistri received branches ranging from 8 to 12 from the auricular surface and 6 to10 from the atrial surface. It was determined that there were more branches taken from the auricular surface and they were stronger. Similar to the study's findings, the literature has reported (Gürbüz, 2015) that the strongest branch is the vena marginis ventricularis sinistri draining ventriculus sinister.

Barszcz et al. (2020) reported that vena cordis media began its course with its two branches getting together; following the study's findings, the first branch was the vena apicis cordis coming from the auricular surface direction. Unlike the study findings, some studies in the literature (Beşoluk and Tıpırdamaz, 2001; Aydınlık et al., 2008; Aksoy et al., 2009, Gürbüz, 2015) did not mention the vena apicis cordis. Similar to the study's findings, Gürbüz (2015) determined that the vena cordis media moved towards the basis cordis within the sulcus interventricularis subsinosus as vena interventricularis subsinosus.

Many domestic animal studies detected vena cordis media (Dursun, 1994; König and Liebich, 2009). Sinus coronarius sometimes directly opens into the atrium dextrum in cattle (Nickel et al., 1981) and European bison (Barszcz et al., 2020). In this study we observed that the vena cordis media opened into the sinus coronarius, unlike European bison (Barszcz et al., 2020), and cattle (Nickel et al., 1981). Similar to the Gürbüz's (2015) findings, it was observed that the branches draining the ventriculus dexter, ventriculus sinister, and septum interventriculare opened into the vena cordis media.

Similar to the literature findings (Yadm and Gad, 1992; Tıpırdamaz et al., 1999; Beşoluk and Tipırdamaz, 2001, Aksoy et al., 2009), in the study it was found that vv. cordis dextra was the vein responsible for venous drainage of the facies atrialis of the heart, and this vein ended by opening into the atrium dextrum. Unlike the findings of this study, Gürbüz and Aksoy (2020) in five Hemshin sheep, reported that there was no vena semicircumflexa dextri. This study determined that the vena semicircumflexa dextri was present, similar to some literature findings (Nickel et al., 1981; Aksoy et al., 2009; Kabak and Onuk, 2012). Similar to the findings of this study, Tıpırdamaz et al. (1999), Aksoy et al. (2009), and Gürbüz (2015) reported that the vena distalis ventriculi dextri opened directly into the atrium dextrum. As Gürbüz (2015) reported in eight Tuj and two Hemshin sheep, the vena coni arteriosi and vena proximalis ventriculi dextri merged to form a common root and opened into the vena semicircumflexa dextri.

CONCLUSION

In this study we found that vena cordis magna, vena cordis media, and vv. cordis dextra were the main veins responsible for the venous drainage of the heart. However, some morphologic differences of the heart vein were determined in Southern Karaman sheep than other species in the literature. The differences were as follows;

- Sinus coronarius was a continuation of vena azygos sinistra, and it was opening into vena cava caudalis.
- Vena collateralis sinister intermedia was as strong as vena collateralis sinister proximalis.
- Vena distalis ventriculi sinistri was opening into vena circumflexus sinister,
- The vena apicis cordis was absent.
- The vena cordis media was opening into the sinus coronaries.
- The vena semicircumflexa dextri was present.

ACKNOWLEDGMENTS

Conflict of Interests: The authors declared that there is no conflict of interests.

Financial Disclosure: The authors declared that this study has received no financial support.

Author's Contributions:
HK and ZÖ designed the study. HK and ZÖ performed surgeries. HK participated in drafting and revising the manuscript. HK: Hülya Kara, ZÖ: Zekeriya Özüdoğru

REFERENCES

Aksoy G, Karadag H, Ozudogru Z. Morphology of the venous system of the heart in the Van cat. Anat Histol Embryol. 2003; 32:129–33.

Aksoy G, Karadag H, Soyguder Z. A macroanatomic investigation on the cardiac veins in the domestic cat. J Health Sci Univ Firat. 2001; 15:315–324.

Aksoy G, Özmen E, Kürtül İ, Özcan S, Karadağ H. The venous drainage of the heart in the Tuj sheep. Kafkas Üniv Vet Fak Derg. 2009; 15(2):279-286.

Aycan K, Bilge A. Plastik enjeksiyon ve korozyon metodu ile vasküler sistem anatomisinin araştırılması. Erciyes Ü Tıp Fak Derg. 1984; 6(4):545-552.

Aydınlık E, Aycan K, Ekinci N. Akkaraman koyununda koroner venlerin anatomisi. Sağlık Bilimleri Dergisi (Journal of Health Sciences). 2008; 17(1):40-45.

Barone R. Anatomie comparée des mammifères domestiques, Angiologie. Paris: Vigot; 2011.

Barszcz K, Polguj M, Goździewska-Harłajczuk K, Klećkowska-Nawrot J. Gross anatomy of coronary veins of the European bison (*Bison bonasus*). BMC Veterinary Research. 2020; 16:38

Bartyzel BJ, Charuta A, Barszcz K, Koleśnik A, Kobryń H. Morphology of the aortic valve of *Gallus gallus f. domestica*. Bull Vet Inst Pulawy. 2009; 53:147-151.

Beşoluk K, Tipirdamaz S. Comparative macroanatomic investigations of the venous drainage of the heart in Akkaraman sheep and Angora goats. Anat Histol Embryol. 2001; 30:249-252.

Budras KD, Habel RE. Bovine anatomy. An illustrated text. Schlütersche, Hannover; 2003.

Budras KD, Röck S. Atlas der Anatomie des Pferdes. Schlütersche, Hannover; 2009.

Constantinescu GM. Guide to regional ruminant anatomy based on the dissection of the goat. Lowa State University Press; 2001.

Dursun N. Veteriner Anatomi II. 1. baskı. Ankara: Medisan Yayınevi; 1994.

Ertuğrul M, Dellal G, Soysal İ, *et al.* Türkiye yerli koyun ırklarının korunması. Uludag Universitesi Ziraat Fakultesi Dergisi. 2009; 23(2):97-119.

Evans HE, Christensen GC. Miller's anatomy of the dog. New York: W. B. Saunders Company; 1993. p.633-651.

Genain MA, Morlet A, Herrtage M, et al. Comparative anatomy and angiography of the cardiac coronary venous system in four species: human, ovine, porcine, and canine. J Vet Cardiol. 2018; 20(1):33-44.

Gürbüz İ. Tuj ve Hemşin Koyunlarında Kalp ve Koroner Damarlar Üzerine Karşılaştırmalı Makroanatomik Araştırmalar [Doktora Tezi]. Kars: Kafkas Üniversitesi; 2015. **Gürbüz İ, Aksoy G.** Venae Cordis and myocardial bridges on the venae. Agric Vet Sci. 2020; 4(2):55-70.

Hagensen MK, Abe AS, Falk E, Wang T. Physiological importance of the coronary arterial blood supply to the rattlesnake heart. J Exp Biol. 2008; 211:3588-3593.

Kabak M, Onuk B. Macroanatomic investigation on the venous drainage of the heart in Roe Deer (Capreolus capreolus). Kafkas Univ Vet Fak Derg. 2012; 18(6):957-963.

Kaymakçı M, Taşkın T. Türkiye koyunculuğunda melezleme çalışmaları. Hayvansal Üretim. 2008; 49(2):43-45.

Koch T, Berg R. Lehrbuch der Veterina¨ r-Anatomie, Band III, die grossen Versorgungs- und Steuerungssysteme, 5 Auflage. Stuttgart: Gustav Fischer Verlag Jena; 1993. p. 15-323.

König HE, Liebich HG. Veterinary anatomy of domestic mammals. Stuttgart: Schattauer; 2009.

Kupczyńska M, Barszcz K, Olbrych K, *et al*. Coronary arteries of the European bison (Bison bonasus). Acta Vet Scand. 2015; 57:82.

Nickel RA, Schummer A, Seiferle E. The Anatomy of the Domestic Animals. Berlin and Hamburg: Verlag Paul Parey. 1981. pp.38-70.

Noor NA, Al-Ayat MA, Swielim GA, Alloush GM. Pattern of distribution of the cardiac veins of the heart of goat (*Capra Aegagrus Hircus*) Advan Biol Res. 2015; 9:449-466.

Tıpırdamaz S, Yalçın H, Beşoluk K, Eken E. Ruminantlarda toplardamarlar. Konya: Selçuk Üniversitesi Basımevi; 1999.

Veterinaria, Nomina Anatomica. "International committee on veterinary gross anatomical nomenclature (ICVGAN)." Published by the Editorial Committee, 6th ed., Hannover; 2017.

Yadm ZA, Gad MR. Origin, course and distribution of the venae cordis in the rabbit and goat (comparative study). Vet Med J. 1992; 40:1-8.

Yadm ZA. Origin, course and distribution of the venae cordis in donkey. Assiut Vet Med J. 1993; 28:15-26.

Yoldaş A, Özmen E, Aksoy G. The anatomy of the caediac veins in Storks (Ciconia ciconia). Kafkas Univ Vet Fak Derg. 2013; 19(4):687-692.

Yoldaş A. Devekuşunda (Struthio Camelus) Kalp ve Arterleri Üzerine Makroanatomik Bir araştırma [Doktora Tezi]. Konya: SÜ Sağlık Bilimleri Enstitüsü; 2007.

Original Article https://doi.org/10.47748/tjvr.1074826

TJVR 2022; 6 (1): 27-32

Turkish Journal of Veterinary Research

https://dergipark.org.tr/tr/pub/tjvr

e-ISSN: 2602-3695

Some macromineral and trace mineral levels in milk of different dog breeds

İnci Söğütlü[1] Nizamettin Günbatar[2] Handan Mert[3] Mustafa Cellat[4] Nihat Mert[3]

[1] *Department of Food Establishments and Codex Republic of Turkey Ministry of Agriculture and Forestry, Ankara, Turkey*
[2] *Health Sciences Faculty, Van Yuzuncu Yil University, Van, Turkey*
[3] *Department of Biochemistry, Faculty of Veterinary Medicine, Van Yuzuncu Yil University, Van, Turkey*
[4] *Department of Physiology, Faculty of Veterinary Medicine, Mustafa Kemal University, Antakya, Turkey*

Correspondence: *İnci Söğütlü (incidoganbiyo@hotmail.com)*

Received: 16.02.2022 Accepted: 12.03.2022

ABSTRACT

Objective: In this study, it was planned to examine the mineral levels in the milk of different dog breeds during the lactation period. Calcium (Ca), magnesium (Mg), potassium (K), sodium (Na), copper (Cu), zinc (Zn), manganese (Mn) and iron (Fe) concentrations were analyzed in dog milk.

Materials and methods: In this research 6 Labradors, 6 German Shepherds, 6 Pointers, 5 Turkish Tazis (sighthound), 5 Setters, 7 Malinois, and 5 Golden Retrievers (a total of 40 dogs) of 3 to 4 years of age were used as research materials, all of which were under same management and feeding conditions. All dogs were on diets appropriate for gestation and lactation periods. Adequate milk volume could be collected 2-3 weeks after parturition, and there were no known medical problems. Each day's samples were kept capped and refrigerated after being collected. The concentrations of calcium, magnesium, potassium, sodium, copper, zinc, manganese and iron, were analyzed by using Varian Brand 30/40 model AAS device.

Results: The Ca, K, Na, Zn, Mn and Fe levels of milk samples from different dog breeds had no significant difference. The highest Mg level was determined in Pointer breed milk samples, and the lowest was determined in Setter milk samples. The highest Cu levels among the inspected races were in Labrador milk samples, whereas the lowest levels were determined in Setter breeds.

Conclusion: This data shows that most of the analyzed milk content of different breeds of dogs did not change significantly during the same lactation period, and any present difference could be taken into account when evaluating breeding studies.

Keywords: *Dog, milk, Macro minerals, Trace minerals*

INTRODUCTION

Dog milk is a fluid that contains enough nutrients that are secreted at different times in the milk glands to feed newborn puppies of female dogs, and the puppy is obliged to consume until it is able to feed itself (Ergun and Mert, 1984). Milk is regarded as a basic food substance by nutritionists. It is important for its calcium, phosphorus, and riboflavin (Vit B2) content. It also contains essential amino acids and fatty acids. Certain substances are found only in milk, like lactose, casein, lactalbumin, and lactoglobulin. The energy value of milk differs based on its composition. One liter of 3% fat consumer milk provides 615 kcal energy. The composition of the milk differs based on the environmental conditions in which the lactating animal lives. Dogs reach twice their birth weight in 9 days, perhaps related to the protein content of the dog's milk, which is 7.3%. Humans, on the other hand, reach twice their birth rate within 180

days, and the protein content of human milk is 1.6% (Bremel, 1995).

Some major and trace elements are necessary for mammals in many physiological functions such as bone and cartilage formation, enzymatic reactions, intracellular and extracellular fluid balances, oxygen transport, electron transfer reactions, normal muscle and nerve functions and hormone production. It is reported that imbalances arising from excess minerals or their deficiencies are associated with pathological conditions (Mert et al., 2008).

Na, K, Ca, Mg, Cl, and phosphate are the basic mineral substances in milk, and there are also many trace elements in it (Ergun and Mert, 1984). The trace elements in the milk are mostly ionic and in salt forms. Since their quantities are very small, their presences are investigated spectrometrically. Generally, those with a lower presence than that can be expressed with "mg/kg" are regarded as trace elements. Feeding of the mother affects the amount of trace element levels. The amount may also vary according to the point of time during the lactation period. In contaminations, some metals may pass through the milk and can change the actual amount. Some trace elements have vital preservation roles and are called micronutrient elements. Micronutrients are Iron, Copper, Cobalt, Zinc, and Iodine. Micronutrients are important in nutritional physiology, such as the cobalt taking part in vitamin B12 structure. They are found in the composition of enzymes, and Fe is involved in the structure of catalase and peroxidase enzymes. They may act as enzyme activators or inhibitors as well.

They also take part in certain chemical reactions that take place within milk and milk products, which may cause quality defects. Cu, for example, causes autooxidation of milk fat. The trace elements are found in the coenzymes (prosthetic group) of the enzymes in the milk. Molybdenum, for instance, is involved in the structure of the xanthine oxidase enzyme. They are also influential in the activity of enzymes. For example, Mg^{++}, Mn^{++}, Co^{++}, and Zn^{++} enhance the activity of alkaline phosphatase. When the amount of trace elements increases, they play a catalytic role in chemical and biochemical reactions and have an adverse effect in high quantities. An increase in copper (>10-5 mol) leads to ascorbic acid autooxidation in milk. For this reason, tools and equipment made of copper shouldn't be used (Keen et al., 1982; Bremel, 1995).

In this study, it was aimed to determine the mineral levels in milk samples obtained from different dog breeds.

MATERIALS and METHODS

The study was conducted according to ethical guidelines and under the supervision of Hatay Mustafa Kemal University Local Ethics Committee board (*Decision no: 2022/01-11*). All animal-use protocols were carried out in accordance with Directive 2010/63/EU of the European Parliament and Council of 22 September 2010 on the protection of animals used for scientific purposes (European Union Directive, 2010). In this research 6 Labradors, 6 German Shepherds, 6 Pointers, 5 Turkish Tazis, 5 Setters, 7 Malinois, and 5 Golden Retrievers (a total of 40 dogs) of 3 to 4 years of age were used as research materials, all of which were under the same management and feeding conditions. Depending on the age of the animals and the orientation of the dogs, commercial dog food was used and an individualized feeding program was applied. The composition of this commercial dog food was as follows: crude protein minimum 28%, crude fat minimum 16%, crude cellulose maximum 3% and crude ash maximum 7%. Additionally, all dogs were on diets appropriate for gestation and lactation periods. Adequate milk volume could be collected 2-3 weeks after parturition, and there were no known medical problems. Each day's samples were kept capped and refrigerated after being collected. Within 24 hours after collection of the last day's sample, all samples were transported to the laboratory in a cold chain. Samples were then warmed (+5°C) in a heat block and turned over repeatedly to resuspend any cream layer that had separated. Maximum attention was given to prevent contamination of the mineral matter of the samples (Salisbury and Chan, 1985).

Homogenized milk samples were digested in acid-rinsed glass Pyrex tubes using trace metal–grade concentrated nitric acid for 5 h at 125°C for AAS measurements. The concentrations of calcium, magnesium, potassium, sodium, copper, zinc, manganese, and iron were investigated in dog milk samples during the course of the lactation period. Mineral analyses were performed using Varian Brand 30/40 model AAS device and the Varian GTA-96 graphite tube atomizer with electrothermal atomization method. The measurements were made in automated mode and

were repeated twice (Tayar et al., 1993; Mert et al., 1994).

Statistical analysis

SPSS 22.0 Windows program (evaluation version) was used for statistical analysis of the data. One-way ANOVA test was used for data analysis; Duncan test was used for multiple comparison tests. P<0.05 was considered statistically significant.

RESULTS

The mineral levels of milk samples obtained from different dog breeds are given in Table 1. Ca, K, Na, Zn, Mn and Fe levels were found to have no significant difference among breeds. The highest Mg level was found in Pointer milk samples and the lowest was in Setter milk samples (p<0.001). The highest Cu levels amongst races were found in Labrador (5.14±0.94), Turkish Tazi (5.04±0.48) and German Shepherd (4.98±0.66) breed milk samples, while the lowest levels were determined in Setter (3.97±0.35) and Golden Retriever (4.11±0.66) samples (p<0.001).

Table 1. Some macro and trace minerals levels in milk samples obtained from different dog breeds.

Parameters (mmol/L)	X±Sx							p Value
	Labrador (n=6)	German Shepherd (n=6)	Pointer (n=6)	Turkish Tazi (n=5)	Setter (n=5)	Malinois (n=7)	Golden Retriever (n=5)	
Ca	5.85±1.18	5.03±0.98	4.46±0.77	6.17±1.22	5.45±1.02	5.88±0.98	4.95±0.77	0.073
Mg	0.87±0.11^{a}	0.71±0.09^{bc}	0.89±0.13^{a}	0.77±0.09^{abc}	0.65±0.08^{c}	0.69±0.07^{bc}	0.81±0.08^{ab}	0.001
K	12.65±1.74	10.44±1.44	11.66±1.34	11.55±1.26	12.01±1.08	11.79±1.11	12.46±1.36	0.160
Na	5.02±1.07	4.74±0.99	4.98±0.98	4.56±0.77	4.98±0.67	4.95±1.08	5.13±1.05	0.972
Cu	5.14±0.94^{a}	4.98±0.66^{a}	4.46±0.75^{ab}	5.04±0.48^{a}	3.97±0.35^{b}	4.76±0.45^{ab}	4.11±0.66^{b}	0.027
Zn	44.19±4.64	43.72±3.98	47.18±4.08	41.76±3.65	42.68±3.99	40.92±4.06	46.78±4.14	0.099
Mn	0.18±0.04	0.15±0.03	0.23±0.05	0.20±0.02	0.22±0.06	0.19±0.04	0.18±0.03	0.053
Fe	6.63±1.21	6.88±1.32	7.04±1.34	6.91±1.04	6.42±1.03	6.76±1.12	7.10±1.12	0.969

DISCUSSION

It is important to know which trace elements are required for adequate growth and development during this nutritionally challenging life expectancy since infants usually receive all their nutrition from one type of food. A number of factors affect the trace element content of the milk (Davidson et al., 1994).

Heinze et al. (2014) analyzed the mineral content of homogenized breast-milk in samples digested with concentrated nitric acid (70%), and found the levels of some minerals as; calcium 6.56±1.22 mmol/L, magnesium 0.93±0.18 mmol/L, potassium 15.1±2.1 mmol/L, sodium 6.35±1.4 mmol/L and copper 9.24±1.81 µmol/L, iron 10.0±7.9 µmol/L, manganese 0.21±0.15 µmol/L, rubidium 13.1±2.9 µmol/L, selenium 0.21±0.06 µmol/L, strontium 0.50±0.16 µmol/L, Zinc 66.7±14.4 µmol/L.

Microminerals also called micronutrients or trace elements, have been described physiologically as substances that are less than 0.01% of body weight (Ergun and Mert, 1984; Mert et al., 1993). This term covers all elements, except for those that make up the organic matrix (carbon, hydrogen, nitrogen, oxygen, and sulfur), as well as body minerals of biological fluids and skeletons (calcium, magnesium, potassium, sodium, chlorine and phosphorus). Iron is the boundary between macroscopic and microminerals and is often processed separately because of its long history and well-documented physiology (Davidson et al., 1994).

Concrete clinical syndromes associated with deficiency of zinc, copper, and iodine are well described (Casey and Walravens, 1988). Iron deficiency does not appear in infants in humans before 6 months due to large deposits of iron at birth (Cavell and Widdowson, 1964; Dallman, 1988). Although specific physiological and/or enzymatic functions can be attributed to molybdenum and manganese, nutritional deficiencies in these elements have not been documented in infants (Casey and Walravens,

1988). The bioavailability of a large number of trace elements that are considered important or important for the growth of a child is available only for iron, zinc, copper, manganese, and selenium.

The concentration of most trace elements in human milk is less dependent on the consumption of the mother or blood (IOM, 1991). Exceptions are "anionic" elements: iodine, fluorine, and selenium. Excessive consumption of many elements, especially those that are metabolized as anions, can be associated with a risk of toxicity for the infant, and strengthening of the suckling mother in terms of these elements is usually not recommended.

The concentration of iron in the milk in most of the domestic animals are in the range of 0.2-1.0 pg/mL at slightly higher levels than in the colostrums. Lonnerdal et al. (1982) reported that about 20% of iron was found to have fat content in the milk and 30-60% in the casein fraction. Iron levels in other animals are as follows: cows 0.2-0.6 μg/mL, buffalo 0.2-0.3 μg/ml, goat 0.3-0.4 μg/mL (Lonnerdal et al., 1981; Kincaid and Cronrath, 1992).

Zinc is an important component of more than 200 enzymes that can act both catalytically and structurally (Hambidge et al., 1986; IOM, 1991). It seems that it plays a critical role in the expression of genes as well: many DNA-binding proteins are zinc complexes. Zinc metalloproteins are also important for protecting the integrity of cell membranes and extracellular matrix architecture (Waxman and Wasan, 1992). Depending on the extent of zinc depletion, deficits in young mammals can lead to delayed growth, anorexia and severe diarrhea and skin lesions (Hambidge et al., 1986; Casey and Walravens, 1988). Due to higher growth rates in men and premature babies, the demand for zinc is increased and they are more vulnerable to deficits (Krebs and Hambidge, 1986). Zinc is found in three main fractions of milk; fat, casein and whey, in various chemical forms. The concentration of zinc is higher in colostrum, which decreases during lactation. Zn concentrations in dogs ranged from 7 to 8 (μg/mL) according to Anderson et al. (1991) and Lonnerdal et al. (1981) whereas in cats it is 5-7 (μg/mL) according to Keen et al. (1982).

Copper is a component of many metalloenzymes such as cytochrome oxidase, superoxide dismutase, ceruloplasmin, enzymes that play a role in the transport of copper into tissues and in the release of iron and in the synthesis of connective tissue, melanin, and catecholamines (Casey and Walravens, 1988). The deficiency of copper as a result of malnutrition is observed in humans and other species, especially amongst young members. Interaction with excess molybdenum and sulfate may be important in the etiology of copper deficiency in pastoral animals. In general, insufficiency in young mammals causes anemia, anorexia, diarrhea, bone disorders, and defects in cartilage, hair growth, and pigmentation (Davis and Mertz, 1987). In many newborns, including humans, the concentration of copper in the liver is higher than in adults, except for sheep. In humans and mice, the level of fetal liver copper can reach up to 10 times in comparison with adults. This copper is closely related to intracellular metallothionein. In all species, the levels in the colostrum are higher but are reduced after a period of lactation. The drop in the copper amount in milk is usually less than the drop in the zinc level, however, a significantly higher percentage, 30-40% of copper in animal milk, is found associated with casein, compared to human milk. In companion animals, the levels are usually an order of magnitude higher than in other animals. In canine milk, the concentration of Cu is 1.3-2 (μg/mL) according to Anderson (1991) and Lonnerdal et al., (1981). In cats, the Cu amount is 0.8-1.2 (μg/mL) according to Keen et al (1982).

Metalloenzymes of manganese have a wide range of metabolic functions: synthesis of mucopolysaccharides, gluconeogenesis, lipid metabolism, neurotransmitters and synthesis of mitochondrial superoxide dismutase at the same time. Manganese deficiencies have been obtained experimentally in several species, but are naturally found in pig and poultry diets, yet have never been found in some people (Hurley and Keen, 1987). Fetal life and premature infancy are the most sensitive periods of manganese deficiency. In dogs, the Mn amount in milk is about 140 (ng/mL), but in colostrum, it was measured approximately 160 (ng/mL) by Lonnerdal et al. (1981).

The main ionic constituents of milk are monovalent ions of sodium, potassium and chloride, and bivalent calcium, magnesium, citrate, phosphate and sulfate ions. Monovalent ions of sodium, potassium, and chloride are amongst the most prevalent minerals in milk, collectively contributing 30 mOsm or a tenth of the total osmolarity of human milk, 82 mOsm or a quarter of the osmolarity of bovine milk, and 196 mOsm or almost two-thirds of the osmolarity of rabbit milk

(Peaker, 1977). Significant changes in concentrations of basic monovalent cations in milk are associated with conditions that facilitate the close bonds between epithelial cells. The main pathological process that changes the content of a monovalent cation in milk is mastitis or localized breast tissue inflammation. Inflammation opens connections between cells, and changes in sodium and chloride content can be determined by measuring the electrical conductivity of milk from animals with mastitis (Linzell and Peaker, 1971). In general, changes in concentration are not associated with systemic diseases, such as diabetes (Butte et al., 1987), cystic fibrosis or local diseases such as mastitis. Some effects on calcium and magnesium have been observed by some authors (Lonnerdal, 1986a; Lonnerdal, 1986b). There are few reports that claim pharmacological doses of magnesium sulfate increase the magnesium concentration in colostrum (Cruikshank et al., 1982). Dietary and seasonal effects on the concentration of calcium and citrate in bovine milk have been reported by Halt and Muir (1979). As the serum citrate increases, calcium increases markedly in the first few days after birth, and then slowly drops to 6.6 mmol/L in the first 3 months after birth. After 3 months, calcium level slowly and consistently falls. Iron, zinc, copper, and magnesium concentrations decrease during lactation, whereas calcium and phosphorus concentrations increase.

During the first 45 days of lactation, iron, copper, zinc, manganese, calcium, magnesium, protein, carbohydrate and fat content of dogs were analyzed. The concentration of iron significantly decreased from 13 μg/mL to 0 to 6 μg/mL. The concentration of zinc is reduced from 9.6 μg/ml to 8.7 μg/mL. During early lactation, the calcium concentration increased from 1.366 μg/mL to 1.757 μg/ml on day 10 but then changed slightly. Concentrations of copper, manganese, magnesium, and carbohydrates did not show strong developmental structures; the mean values were 1.8 μg/mL, 0.14 μg/mL, 59 μg/mL and 4.5%, respectively (Lonnerdal et al., 1981).

CONCLUSION

The concentrations of calcium, magnesium, potassium, sodium, copper, zinc, manganese and iron were analyzed in dog milk during the course of lactation. The Ca, K, Na, Zn, Mn and Fe levels of milk samples from different dog breeds were found to have no significant difference. The highest Mg levels were determined in Pointer milk samples and the lowest levels were found in Setter milk samples. The highest Cu levels amongst races were found in Labrador milk samples whereas the lowest levels were determined in Setters. These data show that milk mineral content of different breeds of dogs should be taken into account in nutritional studies.

ACKNOWLEDGMENTS

Conflict of Interests: The authors declared that there is no conflict of interests.

Financial Disclosure: The authors declared that this study has received no financial support.

Author's Contributions: İS, NM and HM designed the study; NG and MC supervising and consulting; MC and İS collecting data and processing; NM, HM, and İS: data analysis and literature review; NM, HM, and İS: writing of the article; NG: critical review. İS: İnci Söğütlü, NM: Nihat Mert, HM: Handan Mert, NG: Nizamettin Günbatar, MC: Mustafa Cellat

REFERENCES

Abram Anderson RS, Carlos GM, Robinson IP, *et al.* Zinc, copper, iron and calcium concentrations in bitch milk. J Nutr. 1991; 121(11):81-82.

Bremel RD. Handbook of milk composition. 1st ed. Cambridge: Academic Press; 1995.

Butte NF, Garza C, Burr R, *et al.* Milk composition of insulin-dependent diabetic women. JPGN. 1987; 6(6):936-941

Casey CE, Walravens PA. Trace elements. In: Tsang RC, Nichols BL, eds. Nutrition During Infancy. Philadelphia: Hanley & Belfus; 1988. p.190-215.

Cavell PA, Widdowson EM. Intakes and excretions of iron, copper, and zinc in the neonatal period. Arch Dis Child. 1964; 39(207):496-501.

Cruikshank DP, Varner MW, Pitkin RM. Breast milk magnesium and calcium concentrations following magnesium sulfate treatment. Am J Obstet Gynecol. 1982; 143(6):685-688.

Dallman PR. Nutritional anemia of infancy: iron, folic acid, and vitamin BI2. In: Tsang RC, Nichols BL, eds. Nutrition During Infancy. Philadelphia: Hanley and Belfus; 1988. p.216-235.

Davidson L, Kastenmayer P, Yuen M, Lonnerdal B, Hurrell R. Influence of lactoferrin on iron absorption from human milk in infants. Pediatr Res. 1994; 35(1):117-124.

Davis GK, Mertz W. Copper. In: Mertz W, eds. Trace Elements in Human and Animal Nutrition. San Diego: Academic Press; 1987. p.301-364.

Ergun H, Mert N. Biochemical changes due to mastitis in milk. I. Mastitis Seminar. Ankara Univ Vet Fak. 1984; 46-61.

European Union Directive. Directive 2010/63/EU of the European Parliament and of the Council of the protection of animals used fer scientific purposes. Official Journal of the European Union. 2010; 276:33-79.

Halt C, Muir DD. Inorganic constituents of milk: I. Correlation of soluble calcium with citrate in bovine milk. J Dairy Res. 1979; 46(3):433-439.

Hambidge KM, Casey CE, Krebs NF. Zinc. In: Mertz W, eds. Trace Elements in Human and Animal Nutrition. 5th ed. Orlando: Academic Press; 1986. p.1-138.

Heinze CR, Freeman LM, Martin CR, *et al*. Comparison of the nutrient composition of commercial dog milk replacers with that of dog milk. J Am Vet Med Assoc. 2014; 244(12):1413-1422.

Hurley LS, Keen CL. Manganese. In: Mertz W, eds. Trace Elements in Human and Animal Nutrition. 5th ed. San Diego: Academic Press; 1987. p.185-223.

Institute of Medicine (IOM). Nutrition during lactation. Subcommittee on Lactation., Committee on Nutritional Status during Pregnancy and Lactation, Food and Nutrition Board, Institute of Medicine, National Academy of Sciences. Washington: National Academy Press; 1991.

Keen CL, Lonnerdal B, Clegg MS, *et al*. Developmental changes in composition of cats' milk: Trace elements, minerals, protein, carbohydrate and fat. J Nutr. 1982; 112(9):1763-1769.

Kincaid RL, Cronrath JD. Zinc concentration and distribution in mammary secretions of peripartum cows. J Dairy Sci. 1992; 75(2):481-484.

Krebs NF, Hambidge KM. Zinc requirements and intakes of breast-fed infants. Am J Clin Nutr. 1986; 43(2):288-292.

Linzell JL, Peaker M. Early detection of mastitis. Vet Rec. 1971; 89:393-394.

Lonnerdal B, Keen CL, Hurley LS, Fisher GL. Developmental changes in the composition of Beagle dog milk. Am J Vet Res. 1981; 42(4):662-666.

Lonnerdal B, Keen CL, Hurley LS. Trace elements in milk from various species. In: Howell McC, Hawthorne JM, White CL, eds. Trace Element Metabolism in Man and Animals, TEMA-4. South Australia: Netley, Griffen Press; 1982. p.249-252.

Lonnerdal B. Nutrition and lactation. In: Hamosh M, Goldman AS, eds. Human Lactation 2: Maternal and Environmental Factors. New York: Plenum Press; 1986a.

Lonnerdal B. Effects of maternal dietary intake on human milk composition. J Nutr. 1986b; 116(4):499-513.

Mert H, Mert N, Doğan İ, Cellat M, Yaşar S. Element status in different breeds of dogs. Biol Trace Elem Res. 2008; 125(2):154-159.

Mert N, Tayar, M, Şen C, *et al*. Determination of Lead (Pb) levels in milk consumed in Bursa region. EU Faculty of Sci. 1994; 12(1):173-176.

Salisbury CD, Chan W. Simple automated wet digestion of animal tissues for determination of seven elements by atomic absorption spectroscopy. J Assoc Off Anal Chem. 1985; 68(2):218-219.

Peaker M. The aqueous phase of milk: Ion and water transport. Symp Zool Soc Lond. 1977; 41:113-134.

Tayar M, Mert N, Çetin M, *et al*. Liver lead levels of slaughtered cattle in Bursa. U U Veteriner Fak Dergisi. 1993; 16(1):16-20.

Waxman J, Wasan H. The architecture of cancer. Br Med J. 1992; 305:1306-1307.

Case Report https://doi.org/10.47748/tjvr.1027439

TJVR 2022; 6 (1): 33-36

Turkish Journal of Veterinary Research

https://dergipark.org.tr/tr/pub/tjvr

e-ISSN: 2602-3695

A case of penile urethral diverticulum in a male crossbreed kid

Ali Belge[1] Rahime Yaygingül[1] Onur Özgün Derincegöz[2]

[1] *Department of Surgery, Faculty of Veterinary Medicine, Aydin Adnan Menderes University, Aydin, Turkey*
[2] *Vet Academia Veterinary Clinic, Izmir, Turkey*

Correspondence: *Ali Belge (abelge@adu.edu.tr)*

Received: 24.11.2021 Accepted: 14.01.2022

ABSTRACT

A 19-day-old, male crossbreed kid with complications of difficulty in urination was referred to the Veterinary Teaching Hospital, Aydin Adnan Menderes University. A purple thin-walled, fluid-filled structure was noticed on the ventral midline and was associated with the prepuce. The cystic structure was sharply incised, and the incision was extended from the most cranial to the most caudal extent of the dilatation. Penile urethral diverticulectomy was performed by the guidance of the urethral catheter. Postoperative attempts at urination resulted in free-flowing streams, and the kid did not have strangury. Sutures and urethral catheter were removed 10 days after surgery.

Keywords: *Kid, Dysuria, Diverticulectomy, Urethral diverticulum*

INTRODUCTION

A Reproductive anomaly in farm animals are frequently reported. Conditions of pseudohermaphrodism, gonadal hypoplasia and aplasia, and various segmental hypoplasias and deformities have been recognized (Rousseaux and Ribble, 1988; Omidi et al., 2011; Bodh and Jadon, 2017; Ali et al., 2020). The common anomalies seen are hypospadias, patent urachus and renal agenesis in goats. These anomalies are usually present in multiples and are often seen with anomalies of other systems (King et al., 2002, Almubarak et al., 2016). Most congenital defects have no clearly established cause; others are caused by genetic or environmental factors or a combination of both; in many cases, the causes are unknown (Blood et al., 1983).

Urethral diverticulum is a condition in which a variably sized "pocket" or outpouching forms next to the urethra and it is either congenital or acquired (Blood et al., 1983; Karras et al., 1992; Anderson et al., 1993). Urethral diverticulum is observed at the pre and post scrotal spot in animals, and emerges as a result of the transient urethral obstruction, or much less frequently due to bacterial urethritis of the lower urinary section (Anderson et al., 1993; Gasthuys et al., 1993).

The present case report aimed to evaluate the surgical treatment outcomes of the penile urethral diverticulum in a male crossbreed kid.

CASE HISTORY

A 19-day-old, male crossbreed kid was brought to the Surgery Clinic, Faculty of Veterinary Medicine, Aydin Adnan Menderes University, with incontinence and dysuria since birth. The owner noticed that the animal has poor sucking reflex, was vocalizing and straining during urination, and has swelling on the prepuce area. Clinical examination of the kid revealed a purple thin-walled, fluid-filled structure on the ventral midline associated with the prepuce (Figure 1A). Exteriorization of the penis was possible. During

the examination, dribbling of small amount of urine was observed.

Figure 1. Penile urethral diverticulum on the preputial region (A), The appearance of kid with congenital penile urethral diverticulum prior to surgery (B), Penile urethral diverticulectomy by the guidance of the urethral catheter (C), The appearance of kid with congenital penile urethral diverticulum after to surgery (D).

The urethral process and glans penis were freed with gentle caudal traction of the prepuce. Exploratory puncture gave urine. It was tender when the diverticular swelling was pressed where urine came from the normal urethral opening. Heart rate, respiratory rate and rectal temperature were 112/min, 30/min and 39.1°C, respectively. Mucosal membrane color, capillary refill time, appetite and hydration status were normal. Blood values were within physiological ranges.

A lubricated sterile catheter (3.5 F) was placed in the urethra. The operation area was prepared for aseptic surgery. The kid was anesthetized with 0.2 mg/kg xylazine hydrochloride, i.m. (Alfazyne, Egevet, Turkey) and 0.11 mg/kg i.m. ketamine hydrochloride (Alfamine, Egevet, Turkey) by intramuscular injection. The kid was placed in dorsal recumbency on the operating table. Lactated Ringer's solution (2 mg/kg/h) was administered during the operation. The surgical site was prepared aseptically. The urine in the swelling of the diverticulum was evacuated by manipulation (Figure 1B). The cystic structure was sharply incised, and the incision was extended from the most cranial to the most caudal extent of the diverticulum. Penile urethral diverticulectomy was performed by the guidance of the urethral catheter (Figure 1C). Urethra and skin sutured with 4-0 polyglactin 910 (Vicryl) and 4-0 silk (mersilk) in a simple interrupted pattern, respectively (Figure 1D).

Antibiotic (25.000 IU/kg/day, intramuscularly, Penicillin G procaine) was administered for 7 days post-operatively. Post-operative attempts at urination resulted in free-flowing streams, and the kid no longer had strangury. Urethral catheter and sutures were removed 10 days post-surgery. The surgical wound healed without any complications.

DISCUSSION

Abnormalities of the reproductive system are common in farm animals, and more common in goats than in sheep. Congenital or hereditary urethral anomalies include urethral stenosis, urethral agenesis, urethral diverticula, urethrorectal fistula, imperforate urethra and urethral duplication, (Wolfe, 1986; Rousseaux and Ribble, 1988; Weaver et al., 1992; Sylly et al., 2019). Urethral dilatation in goats can be combined with congenital anomalies such as hermophradismus,

cryptorchism and dilatation of vesica urinaria (Sylly et al., 2019). The congenital urethral diverticulum was reported in a goat (Karras et al., 1992). Temizsoylu (2005) reported congenital urethral diverticulum and phimosis in male a kid. Sindak et al. (2010) reported urethral dilatation, ectopic testis, hypoplasia penis, phimosis in a Kilis goat kid. In this case, clinical examination revealed a purple thin-walled, fluid-filled structure on the ventral midline associated with the prepuce. The urethral diverticulum was diagnosed according to clinical findings and this defect was also congenital. Urine stasis in the dilated portion of the urethra may result in bacterial urethritis from ascending infections. Excision of the urethral dilatation or perineal urethrostomy should be considered if an infection is refractory to conservative management (Karras et al., 1992; Anderson et al., 1993; Gasthuys et al., 1996; Sylly et al., 2019). The condition is generally associated with urethritis and/or cystitis as a result of an accumulation of urine in the swelling for a long period and even rupture of the urinary bladder may ensue if the condition was associated with aplasia of the penis (Anderson et al., 1993; Javdani et al., 2009). We did not encounter any signs of urethritis or cystitis and the penis and scrotum were normal in our case.

Magda and Youssef (2009) reported urethral diverticulum in 7 kids. The penile urethral diverticular extension was ovoid in four cases and ovoid with multiple swellings pre and post scrotal in two cases. In our case, the penile diverticulum was ovoid and swelling was ventrally located at pre scrotal region.

Previous studies have reported that local swelling in urethral dilatation has a fluctuant character (Temizsoylu, 2002; Magda and Youssef, 2009;). Urination is achieved by pressure on swelling and is painful. Our findings were in agreement with those demonstrated symptoms.

Urethral structures in small ruminants are usually treated by amputation or prophylactically (Fuller et al., 1992; Karras et al., 1992; King et al., 2002; Cruz-Arambulo et al., 2003). Treatment of such cases was directed towards surgical correction when it is possible (Karras et al., 1992), otherwise, perineal urethrostomy or penile resection is indicated if an infection is refractory to conservative management. Several researchers (Anderson et al., 1993; Temizsoylu, 2005; Sedeek and Bakr, 2009) had suggested excision and perineal urethrostomy for the treatment of urethral diverticulum. Temizsoylu (2005) treated urethral dilatation by urethrostomy; and phimosis by amputation of narrowed preputium. Sindak et al. (2010) treated urethral dilatation by urethrostomy in the male goat kid. They considered no treatment for hypoplasia penis, phimosis and ectopic testis due to infertility. Sedeek and Bakr (2009) performed perineal urethrostomy and partial resection of the penis including the dilated urethra. In the present case report, the urethral diverticulum in the male goat kid was treated by urethrostomy.

CONCLUSION

In conclusion, in the present report, the urethral diverticulum was surgically treated using excision and urethrostomy successfully. No complications were seen next days.

ACKNOWLEDGMENTS

Conflict of Interests: The authors declared that there is no conflict of interests.

Financial Disclosure: The authors declared that this study has received no financial support.

Author's Contributions: AB, RY and OÖD designed the study. AB, RY and ÖOD performed surgeries. AB and RY participated in drafting and revising the manuscript. AB: Ali Belge, RY: Rahime Yaygingül, OÖD: Onur Özgün Derincegöz

REFERENCES

Ali MM, Hussein KH, Sadek A, Abdelbaset AE. Congenital urethral dilatation in cattle calves: Diagnosis and surgical intervention. Vet World. 2020; 13(2):261.

Almubarak AM, Abdelghafar RM, Gameel AA, Osman NM. Penile urethral hypospadias with two fistulae and diverticulum in a Saanen kid. Case Rep Vet Med. 2016; 1-3.

Anderson DE, Wallace CE, Williamson L, Mahaffey MB. Urethral recess dilatation in a charolais-cross bull calf. Can Vet J. 1993; 34(4):234-235.

Blood DC, Radostits OM, Henderson JA. Veterinary medicine. 6th ed. London: Bailliere Tindall; 1983. pp.366-367.

Bodh D, Jadon NS. Surgical Management of Penile Urethral Diverticulum in a Kid. Intas Polivet. 2017;18(2):413-414.

Cruz-Arambulo RJ, Tan L, Callan RJ, Van Metre DC, Park RD. What is your diagnosis? (Communication between the urethra and corpus spongiosum, urethral stricture mild cystitis, and presence of a urethral diverticulum). J Am Vet Med Assoc. 2003; 222:1211-1212.

Fuller DT, Baird AN, Morris EL, Kraemer DC. What is your diagnosis? (Hypospadias and urethral diverticulum in goat). J A Vet Med A. 1992; 201:1431-1432.

Gasthuys F, Martens A, De Moor A. Surgical treatment of urethral dilatation in seven male cattle. Vet Rec. 1996; 138:17-19.

Gasthuys F, Steenhaut M, De Moor A, Sercu K. Surgical treatment of urethral obstruction due to urolithiasis in male cattle: a review of 85 cases. Vet Rec. 1993; 133:522-526.

Javdani GM, Dehghani NS, Raayat JAR. Congenital penile urethral aplasia in a 4-day-old calf. Iran J Vet Res. 2009; 10:87-89.

Karras S, Modransky P, Welker B. Surgical correction of urethral dilation in an intersex goat. J Am Vet Med Assoc. 1992; 201:1584-1586.

King WW, Young ME, Fox ME. Multiple congenital genitourinary anomalies in a polled goat. Contemp Top Lab Anim Sci. 2002; 41(5):39-42.

Magda MA, Youssef HA. Surgical management of congenital malformations in ruminants. Avaiable at: http://www.priory.com/vet/congenital_malformations_ruminants.htm, Accessed July 14, 2009.

Omidi A, Monjezi S, Nabipour A. Hypospadias, diverticulum, and agenesis in the penile shaft of a goat kid (Capra hircus). Comp Clin Path. 2011; 20(4):417-419.

Rousseaux CG, Ribble CS. Developmental anomalies in farm animals II defining etiology. Can Vet J. 1988; 29:30-39.

Sylla L, Crociati M, Pistolesi A, Pisello L, Caivano D, Angeli G. Urethrostomy in an Alpine kid secondary to congenital penile urethral diverticulum. Large Anim Rev. 2019; 25(4):153-156.

Sedeek AM, Bakr HA. Comparison between urethrostomy and penile resection for treatment of congenital penile urethral dilatation in calves. J Vet Med. 2009; 19:1-6.

Sindak N, Sahin T, Selçukbiricik H. Urethral dilatation, ectopic testis, hypoplasia penis, and phimosis in a Kilis goat kid. Kafkas Univ Vet Fak Derg. 2010; 16:147-150.

Temizsoylu MD. Penile urethral diverticulum in a kid. Ankara Univ Vet Fak Derg. 2005; 52:185-187.

Weaver AD, Johnson GC, Hill J. Congenital megalourethra in a male Charolais calf. Can Vet J. 1992; 33:270-272.

Wolfe DF. Surgical procedure of the reproductive system of the bull. In: Morrow DA (Ed.), Current Therapy in Theriogenology 2. 2nd ed. Philadelphia: WB Saunders Co; 1986. pp.353-397.

TURKISH JOURNAL OF VETERINARY RESEARCH
E-ISSN:2602-3695

INSTRUCTIONS FOR AUTHORS

General Considerations

TJVR strictly obeys the recommendations of the ICMJE, WAME and flowcharts of COPE.

During manuscript application process "Copy Right Transfer Form" signed by all the researchers in the study should be uploaded to the system.

In studies where "Ethical Approval Document" is needed, the relevant document should be scanned in the browser and transferred to the system at the application stage.

Our journal is incorporate the ICMJE recommendations into our review and publication process.

New Manuscript Submissions

Submit manuscripts through the journal's online system. To begin, go to *Manuscript Submission Page* at the following link:

https://dergipark.org.tr/en/journal/1986/submission/step/manuscript/new

Manuscript Categories

Original Research: An Original Research article is a research paper that provides new information derived from original data and usually includes extensive statistical analysis.

Review Article: A Review Article is an in-depth analysis of the current status of a particular topic. It is not an original article with new data but represents a well-balanced summary of a timely subject with reference to the literature.

Letter to the Editor: A Letter to the Editor offers brief comments on published material and should be objective, constructive, and educational.

Case Report: A Case Report is a brief description of a single unique or unusual case. The manuscript should include a title, authors' full names, degrees, and affiliations, a brief text description/discussion without headings, up to 10 references if applicable, and figure legends; note that each figure part (ie, Figure 1A or 1B) is counted as a separate image. No more than 4 images total may be included. It should not contain tables or data analysis. Case Report are generally not peer reviewed and are published at the discretion of the editor based on space available; publication is not guaranteed.

Short Communication: A Short Communication article is a rather short paper reporting preliminary observations, new interpretations of old data, simple new techniques or devices, or points of historical interest.

Organization of The Manuscript

Manuscripts should be organized in the following order, as applicable: title page, structured abstract or summary (when applicable; letters to the editor, review articles and case reports do not have a

structured abstract), full text, acknowledgments, footnotes, references, tables and figure legends. All text elements and tables should be combined in a single document, double- spaced, with line numbering.

Title Page

This first page should contain the complete title of the article, manuscript category, names and credentials of all authors, institutional affiliations of all authors, orcid (all authors of the manuscript must have a orcid number) of all authors and a short running title (≤60 characters). The corresponding author should be indicated, including a complete e-mail address and telephone number.

Structured Abstract or Summary

An abstract is required for Original Research articles. The abstract should be divided into *Objectives, Materials and Methods, Results, and Conclusions* sections. It should be between 250-350 words. Three to 6 key words should be provided at the end. The abstract should not contain figures, tables, or reference citations, trade names, or manufacturer names. Statements of statistical significance should include 'p' values or 95% confidence intervals. The abstract should not include data that are not given in the full text.

In place of an abstract, a summary is required for Letters to the editor, Review Articles, and Case Reports. Content should adhere to the guidelines for abstracts but should not be divided into sections. It should not exceed 200 words and should give a brief overview of the article. Three to six keywords should be provided at the end. Your keywords must come from the list of approved keywords (MeSH library) maintained by the Medical Subject Headings section of the U.S. National Library of Science or Tü rkiye B ilim Terim leri web page.

Full Text

For Original Research articles, the full text of the manuscript should be divided into the following sections: *Introduction, Materials and Methods, Results, Discussion, Conclusion*. For other articles, the text may be divided into sections if desired. Microsoft Word is preferred. All text should be double spaced, and all text elements, including tables, should be combined in a single document. Manuscripts should include continuous line numbering.

Acknowledgments

On a separate page preceding the references, contributions made by colleagues who are not authors of the paper should be acknowledged. This page should also include acknowledgments of published material reproduced with permission, previous presentations of the work at meetings, related grant support received, and disclosures of relevant commercial interests.

Footnotes

Footnotes are to be used when referencing each of the following types of information:

- Abstracts
- Conference presentations
- Online databases
- Personal communications

- Products, drugs, equipment, and other materials
- Statistical and computer software
- Theses and dissertations

Specific products, equipment, or drugs should be included in the footnotes only if they were essential to the outcome of the report or study. Products, equipment, and drugs that are commonly used materials in veterinary medicine need not be footnoted.

Footnotes should be cited in the text as superscript letters and listed alphabetically after the Acknowledgments section and before the references. If more than 26 footnotes are required, continue the sequence with double letters (eg, aa, bb, and cc). For products and equipment, provide complete information in the footnote, including manufacturer's name and location (ie, city, state, and country).

References

Each reference must be cited with first author's surname and publication year (Ceylan, 2004; Ceylan and Ekin, 2006; Ceylan et al., 2008) in the text.

In references list, when more than 6 authors are included in a reference, ***et al*** replaces the names of all authors after the first 3. Inclusive page ranges should be given where applicable. Accepted work in press includes the journal title or the publisher if it is a book. Material not accepted for publication cannot be included as a reference and should be cited parenthetically in the text as unpublished data, including all participants' initials and surnames and the year. Abbreviations of journal titles should conform to those used in the *National Library of Medicine* (http://www.ncbi.nlm.nih.gov/nlmcatalog/journals). The style and punctuation of references should follow the formats illustrated by the following examples:

Journal Article with Up to 6 Authors

Stephane A, Luo W, Zhou X. Management of congenital cholesteatoma with otoendoscopic surgery: Case Report. Turkiye Klinikleri J Med Sci. 2010; 30(2):803-807.

Journal Article with More Than 6 Authors

Stephane A, Luo W, Zhou X, *et al*. Management of congenital cholesteatoma with otoendoscopic surgery: Case Report. Turkiye Klinikleri J Med Sci. 2010; 30(2):803-807.

Journal Article Published Online Ahead of Print

Cummisford K, Sundar S, Hagberg R, Mahmood F. Realtime three-dimensional transesophageal echocardiography and a congenital bilobar left atrial appendage [published online ahead of print June 24, 2009]. J Cardiothorac Vasc Anesth. doi:10.1053/j.jvca.2009.04.005.

Abstract of a Paper Presented at a Meeting

Shipp TD, Bromley B, Benacerraf BR. Comparison of the fundal endometrial diameters using 3-dimensional rendering for those with embedded and non-embedded intrauterine devices [abstract]. J Ultrasound Med. 2009; 28(suppl):47.

Whole Book

Solcia E, Capella C, Kloppel G. Tumors of the exocrine pancreas. Tumors of the Pancreas. 2nd ed. Washington: Armed Forces Institute of Pathology; 1997. p.145-210.

Edited Book

Underwood LE, Van Wyk JJ. Normal and aberrant growth. In: Wilson JD, Foster DW, eds. Wiliams' Textbook of Endocrinology. 1st ed. Philadelphia: WB Saunders; 1992. p.1079-1138.

Website

Animal and Plant Health Inspection Service. Bovine spongiform encephalopathy (BSE). Available at: www.aphis.usda.gov/lpa/issues/bse/bse.html. Accessed Feb 18, 2003.

Tables

Tables must be numbered consecutively with Arabic numerals in the order in which they appear in the manuscript. Each table should appear on a separate page and should contain a title that includes the table number. No vertical lines or borders may appear in a table. Tables must contain all necessary information so that they may stand alone, independent of the text. Data given in the text should not be duplicated in tables. All tables must be cited in numerical order in the text. Tables should be included in the text document and should not be submitted as graphics.

Figure

For initial submissions, figure legends should be provided at the end of the text document. Figures must be numbered consecutively with Arabic numerals in the order in which the figures appear in the article. All figures should be uploaded in jpeg or tiff format at least 300 dpi resolution with the name of the figure (eg, Figure 1), separately. For figures that include multiple panels, each panel should be sequentially labeled with a capital letter in the same corner of each panel. If a figure contains 2 or more rows of panels, the letter labels should be applied sequentially from left to right in the first row, then from left to right in the second row, and so on. All letters and rows used on the figures should be same size and character.

Similarity Index

Similarity index report, created by ithenticate or Turnitin software, must be uploaded during submission. Our journal expects the similarity index to be less than %25 for submitted manuscripts.

Abbreviations

Abbreviations of common clinical and technical terms listed in the *American Medical Association Manual of Style, 10th Edition*, may be used if they appear 3 or more times in the full text and abstract/summary, respectively. Each abbreviation should be defined at first use in the full text and abstract/summary, respectively. Use of other abbreviations is discouraged unless they are essential to the clarity of the manuscript.

Supplemental Materials

Additional materials that are not in themselves essential to the understanding of the article but provide an important expansion of the article contents may be submitted for publication as supplemental materials. Examples include extended descriptions of experimental methods, extended bibliographies, additional supporting data or results (eg, tables and figures), reporting checklists, copies of survey instruments or questionnaires, handouts, forms, and multimedia representations (eg, video clips) of relevant content.

Supplemental materials must be useful to readers and relevant to the article; redundant and extraneous

content will not be accepted. Whether supplemental materials will be accepted for publication is solely at the discretion of the editors. Supplemental materials accepted for publication will not appear in the printed version of the journal but will be posted on the journal's website. Ideally, supplemental materials will be sent with the manuscript to external reviewers for peer review. Whether supplemental materials have or have not undergone peer review will be indicated on the landing page where the supplemental materials are posted. Supplemental materials should be prepared in compliance with the general guidelines for manuscript style. Although supplemental materials may undergo minor copy editing or formatting, they generally will not undergo the same substantive editing provided for manuscripts. Therefore, the authors are responsible for ensuring clarity and accuracy of the content.

Permission to Reproduce Published Material

Written permission from the author and publisher of any previously published figure, table, or lengthy passage of text included in the manuscript must be submitted with the paper. If any form of preliminary publication, other than an abstract of no more than 400 words, has occurred or is contemplated, a reprint or manuscript of the actual or proposed preliminary publication should accompany the manuscript.

Authority/Responsibility

The intellectual content of the paper is the responsibility of the author; the editor and the TJVR accept no responsibility for the opinions and statements of authors. While every effort is made by the editor and editorial staff to avoid any inaccurate or misleading information, they accept no liability for the consequences of wrong information. The authors agree to keep the editor and publisher fully indemnified against any liability or claim that may arise from the publication of incorrect or misleading data.

Ethics in Experimentation

If the work involves the use of human and animal subjects, the author should ensure that the work described has been carried out in accordance with the internationally accepted rules and codes of conduct. The authors should clearly indicate in the manuscript that such guidelines have been followed and the study has been approved by the appropriate ethical committee along with name of committee and reference code.

Editing

Accepted manuscripts will be copyedited to eliminate grammatical and typographical errors and to ensure conciseness and clarity. The corresponding author will receive proofs of the copyedited article before publication.

Permission Requests

Manuscripts are considered for publication with the understanding that they are submitted solely to the Turkish Journal of Veterinary Research and are not under consideration elsewhere.

CONTACTING THE JOURNAL

The Turkish Journal of Veterinary Research Editorial Office may be contacted through the following:

Prof. Dr. Ebubekir CEYLAN

Ankara Üniversitesi Veteriner Fakültesi

İç Hastalıkları AD Dışkapı, 06110 Ankara, TURKEY

E-mail: *ebubekirceylan@gmail.com*, *infotjvr@gmail.com*

Manuscripts are considered for publication with the understanding that they are submitted solely to the Turkish Journal of Veterinary Research and are not under consideration elsewhere.

TURKISH JOURNAL OF VETERINARY RESEARCH
E-ISSN:2602-3695

Article Copyright Transfer Agreement

We, the undersigned researchers, certify that; the article we have sent; is original, wasn't sent to or disapproved of potential publication by any other journal, has not initially published, and we bear the responsibility concerning the Scientific content and Ethical values related to the article, and transfer any kind and form of copyright related to the Article to Turkish Journal Veterinary Research (TJVR) since it is published in the journal, and accept that we will not make any changes wholly or partly in the article and chose ……..……..…… named author as the authorized researcher.

Title of the article: ……..……..……

……..……..……..……

……..……..……..……

……..……..……..……

	Authors Name	Date	Signature
1.			
2.			
3.			
4.			
5.			
6.			

Authorized Researcher

Title, Name-Surname :

Full Address :

e- mail :

Tel, Fax :

Date and Signature :